Journal of Sedimentary Research

1926 SEPM
Society for Sedimentary Geology

EDIACARAN LIFE CLOSE TO LAND: COASTAL AND SHOREFACE HABITATS OF THE EDIACARAN MACROBIOTA, THE CENTRAL FLINDERS RANGES, SOUTH AUSTRALIA

WILLIAM J. MCMAHON,[*1] ALEXANDER G. LIU,[2] BENJAMIN H. TINDAL,[2] AND MAARTEN G. KLEINHANS[1]

[1]*Faculty of Geosciences, Utrecht University, Princetonlaan 8a, 3584 CB, Utrecht, The Netherlands*
[2]*Department of Earth Sciences, University of Cambridge, Downing Street, Cambridge CB2 3EQ, U.K.*
W.McMahon@hull.ac.uk

ABSTRACT: The Rawnsley Quartzite of South Australia hosts some of the world's most diverse Ediacaran macrofossil assemblages, with many of the constituent taxa interpreted as early representatives of metazoan clades. Globally, a link has been recognized between the taxonomic composition of individual Ediacaran bedding-plane assemblages and specific sedimentary facies. Thorough characterization of fossil-bearing facies is thus of fundamental importance for reconstructing the precise environments and ecosystems in which early animals thrived and radiated, and distinguishing between environmental and evolutionary controls on taxon distribution. This study refines the paleoenvironmental interpretations of the Rawnsley Quartzite (Ediacara Member and upper Rawnsley Quartzite). Our analysis suggests that previously inferred water depths for fossil-bearing facies are overestimations. In the central regions of the outcrop belt, rather than shelf and submarine canyon environments below maximum (storm-weather) wave base, and offshore environments between effective (fair-weather) and maximum wave base, the succession is interpreted to reflect the vertical superposition and lateral juxtaposition of unfossiliferous non-marine environments with fossil-bearing coastal and shoreface settings. Facies comprise: 1, 2) amalgamated channelized and cross-bedded sandstone (major and minor tidally influenced river and estuarine channels, respectively), 3) ripple cross-laminated heterolithic sandstone (intertidal mixed-flat), 4) silty-sandstone (possible lagoon), 5) planar-stratified sandstone (lower shoreface), 6) oscillation-ripple facies (middle shoreface), 7) multi-directed trough- and planar-cross-stratified sandstone (upper shoreface), 8) ripple cross-laminated, planar-stratified rippled sandstone (foreshore), 9) adhered sandstone (backshore), and 10) planar-stratified and cross-stratified sandstone with ripple cross-lamination (distributary channels). Surface trace fossils in the foreshore facies represent the earliest known evidence of mobile organisms in intermittently emergent environments. All facies containing fossils of the Ediacaran macrobiota remain definitively marine. Our revised shoreface and coastal framework creates greater overlap between this classic "White Sea" biotic assemblage and those of younger, relatively depauperate "Nama"-type biotic assemblages located in Namibia. Such overlap lends support to the possibility that the apparent biotic turnover between these assemblages may reflect a genuine evolutionary signal, rather than the environmental exclusion of particular taxa.

INTRODUCTION

Late Ediacaran macrofossils ($\sim$ 574–539 Ma) offer critical information about the early evolutionary history of large and complex multicellular organisms (Linnemann et al. 2019; Matthews et al. 2020). How the Ediacaran macrobiota relate to extant animals, their life habits, and the conditions under which their fossils were preserved are fundamental questions whose answers require an understanding of the environments inhabited by the organisms, evidence of which is archived in the sedimentary record. This study presents revised interpretations of the sedimentary facies and stratigraphic architecture of the siliciclastic Ediacaran-age Rawnsley Quartzite of South Australia, whose eponymous Ediacara Member hosts one of the world's most taxonomically diverse assemblages of the Ediacaran macrobiota (e.g., Droser et al. 2006, 2017; Gehling and Droser 2013; Droser and Gehling 2015). The Ediacara Hills in

the Flinders Ranges, in which Reginald Sprigg originally discovered Precambrian macrofossils (Sprigg 1947), ultimately lent its name to the Ediacaran System (Knoll et al. 2004, 2006). As an important global focal point for studies of Ediacaran life with a long history of research (e.g., Glaessner and Daily 1959), it is essential that the preserved depositional environments of the Rawnsley Quartzite are both well studied and robustly understood.

Detailed accounts of previously proposed facies schemes for the Rawnsley Quartzite have been provided in a number of recent publications and will not be repeated here (e.g., Gehling 2000; Tarhan et al. 2017; Reid et al. 2020). However, it is worth noting that early descriptions of the unit favored intertidal and lagoonal depositional environments for the fossil-bearing facies (Jenkins et al. 1983) (Table 1). Gehling (2000) provided detailed descriptions of the sedimentary facies at a large number of previously undocumented Rawnsley Quartzite sections from across the Flinders Ranges, and reinterpreted the fossiliferous parts of the succession to comprise five facies, four of which were considered to have been

* Present Address: Energy & Environment Institute, University of Hull, Cottingham Road, Hull HU6 7RX, U.K.

TABLE 1.—*Previous paleoenvironmental interpretations of Ediacara Member and upper Rawnsley Quartzite sedimentary facies. Facies numbers at top follow those used in this study. Note that Gehling and Droser (2013) have an additional "mass-flow" facies, in this study interpreted as the product of seismic activity and represented in a number of facies.*

| | FACIES | | | | | | | | |
	1 & 3	2	4	5	6	7	8	9	10
Jenkins et al. 1983	High-energy (beach and barrier complex?)	Intertidal	Lagoon or neritic shelf	Intertidal	Intertidal	Not described	Not described	Not described	Not described
Gehling 2000	Submarine flow	Prodelta	Prodelta	Delta-front Sheet-flow	Delta-front Wave-base	Delta-top Shoreface	Tidal sandflat	Not described	Shallow subtidal
Gehling and Droser 2013	Not described	Delta-front	Delta-front	Delta-front	Delta-front	Not described	Not described	Not described	Not described
Tarhan et al. 2017	Not described	Delta-front or prodelta	Delta-front or prodelta	Subwave-base upper canyon fill	Oscillatory and combined flow	Not described	Not described	Not described	Not described
Reid et al. 2020	Not described	Delta-front or prodelta	Delta-front or prodelta	Sediment gravity flows	Upper wave-base	Shoreface	Not described	Not described	Not described
This study	Tidally-influenced fluvial or estuarine	Mixed-flat	Lagoon?	Lower shoreface	Middle shoreface	Upper shoreface	Foreshore	Backshore	Distributary channels or sandy shoals

deposited below effective (fair-weather) wave base (and three beneath maximum (storm-wave) base) (see Gehling and Droser 2013, their Fig. 1). Since that seminal study, most sedimentological research on the unit has focused solely on fossil-bearing facies, predominantly at one location (Nilpena; Fig. 1; though see Reid et al. 2020). Furthermore, interpretations of Rawnsley Quartzite depositional environments have remained relatively unchanged (Table 1). Our revised environmental framework, presented following fieldwork at five sections in the central and western reaches of the Flinders Ranges (Fig. 1A), considers Gehling's (2000) inferred water depths to be overestimations at these locations. We demonstrate that all observed fossil-bearing facies of the Ediacara Member fall within the marine shoreface complex—the seaward-sloping ramp extending from the low-tide mark to the lower limit of the fair-weather wave base (e.g., Reinson 1984; Pemberton et al. 2012) (Fig. 2), in addition to a number of distinct coastal environments. This finding contrasts with previous studies, which considered the marine shoreface complex to be only scarcely fossiliferous (Gehling and Droser 2013 (their Table 1); Tarhan et al. 2015; Reid et al. 2020).

GEOLOGICAL SETTING

The Ediacaran Rawnsley Quartzite, presently divided in ascending order into the Chace Quartzite Member, The Ediacara Member, and The Upper Rawnsley Quartzite, crops out over an outcrop belt of 20,000 km² in the vicinity of the Flinders Ranges of South Australia (Fig. 1). Following formalization of the Chace Quartzite and Ediacara Member (Jenkins 1975; Reid and Preiss 1999), Gehling (1982, 2000) demonstrated that: 1) the Chace Quartzite Member, for which a sandflat-to-supratidal depositional environment was assigned, is separated from overlying strata by a distinct incised valley (Fig. 1B), and 2) the fossiliferous Ediacara Member comprised all deposits from the base of this valley-contact to the topmost fossiliferous facies. The upper Rawnsley Quartzite was proposed to extend from the first unfossiliferous facies overlying the Ediacara Member to the disconformable contact with overlying Cambrian-age deposits (Fig. 1). Gehling (2000) demonstrated the variable stratigraphic thickness (10–300 m) of the Ediacara Member across the Flinders Ranges (though see discussion in Sequence Stratigraphic Evolution, below) and identified valley-shaped incisions that are occasionally tractable at outcrop (Fig. 1B). Considering its occurrence disconformably beneath a notable erosional hiatus of unknown duration (i.e., an incised sequence boundary), the Chace Quartzite Member should be more appropriately treated as a distinct formation with respect to the rest of the Rawnsley Quartzite. In this study we do not explicitly address the Chace Quartzite Member, and instead focus on the rest of the Rawnsley Quartzite (the Ediacara Member and the Upper Rawnsley Quartzite) at four locations across its central outcrop belt: 1) Brachina Gorge, 2) Bunyeroo Gorge, 3) Moralana, and 4) Wilpena Pound (Figs. 1, 3, 4).

FACIES ANALYSIS

Methodology

We define 10 sedimentary facies based on lithology, primary sedimentary structures, erosional and depositional surfaces, and grain-size trends (Table 2). Paleocurrent directions were measured wherever reliable surfaces were available. Foreset planes were reoriented on a stereonet to remove bedding dip whenever dip angle exceeded 10°. Our ten facies record a complex of estuarine, coastal, and shoreface environments (locally affected by storms). Use of the terms "effective (fair-weather) wave base" and "maximum (storm-weather) wave base" follows the definition used by Reading and Collinson (1996), who placed shelf deposition entirely beneath maximum wave-base, and the offshore regime below effective wave base but above maximum wave base. The shoreface begins at the lower limit of the effective wave base and extends landward until the low-
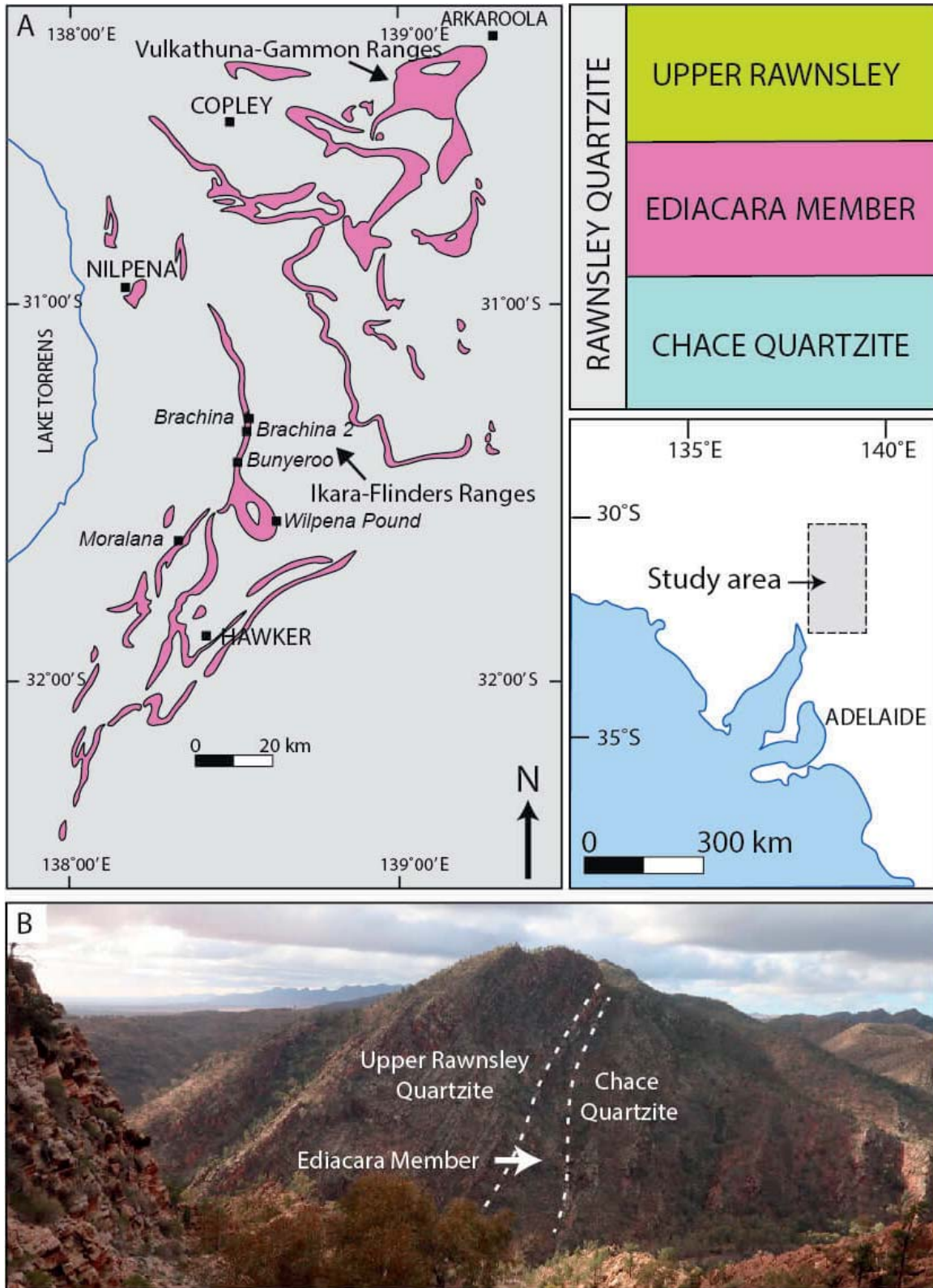
FIG. 1.—**A)** Geographic and stratigraphic context of the Rawnsley Quartzite outcrop belt in South Australia. Purple denotes exposure of Rawnsley Quartzite. Localities forming part of this study are shown in italics. Modified from Gehling (2000). **B)** Preserved Ediacara Member paleovalley. Bunyeroo Gorge. Valley fill is approximately 30 meters thick. Photograph facing 010°.
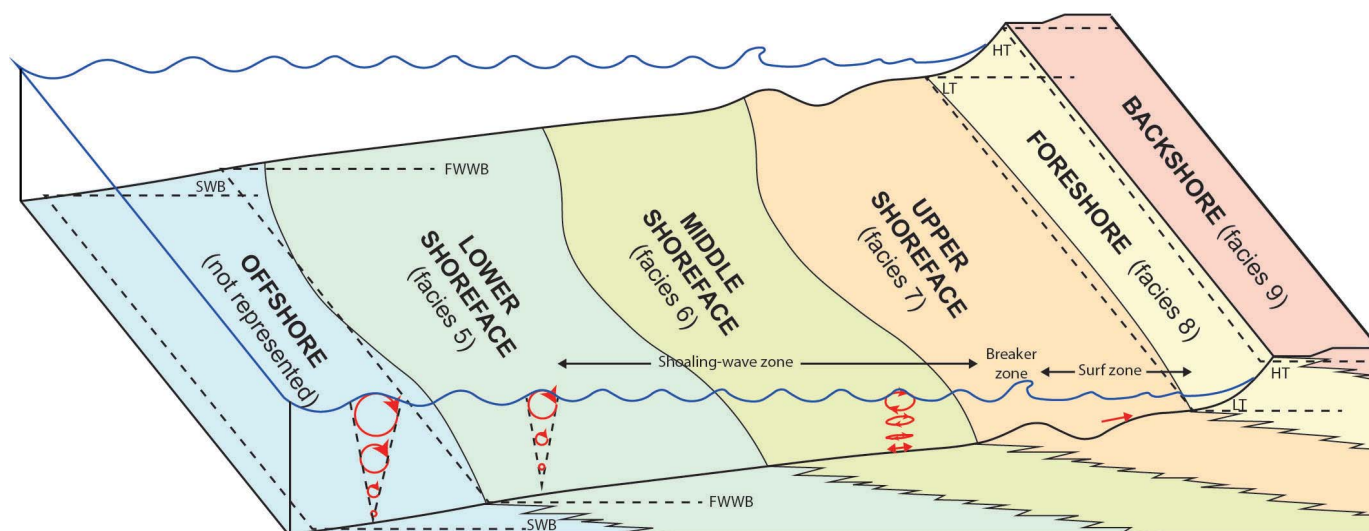
FIG. 2.—Idealized block diagram of the shoreface and beach. The locations of the various shoreface zones, wave zones, fair-weather wave base (FWWB), storm-wave base (SWB), high tide (HT), and low tide (LT) are given. Rawnsley Quartzite facies interpreted to occupy these settings are shown.

tide mark (Fig. 2). The foreshore is restricted to the intertidal realm occupying the area acted on by wave swash, whereas the backshore hosts an amalgam of coeval beach, washover, and supratidal environments. In contrast with preceding work on the Rawnsley Quartzite, deposits below effective (and maximum) wave base are not recognized. Paleontological information provided for each facies is restricted to our own primary observations. Valuable published datasets documenting the facies occurrence of macrofossils in the Rawnsley Quartzite (e.g., Gehling and Droser 2013; Droser and Gehling 2015; Reid et al. 2018; Droser et al. 2019; Evans et al. 2019) are not incorporated into this study due to uncertainties surrounding correlations between facies descriptions. Those datasets also largely originate from the Nilpena locality (Fig. 1), a location not visited in this study.

Facies 1: Basal Cross-Bedded Unfossiliferous Sandstone

Sedimentology.—A dominantly medium- to coarse-grained quartz arenitic sandstone forms the lowermost part of Ediacara Member stratigraphy at Wilpena Pound, Brachina Gorge, and Moralana. Individual beds range from 30 to 510 cm in thickness and contain recognizable channel forms (Fig. 5A). Weathered faces give the sandstone an apparently massive appearance in many outcrops (Fig. 5B), but clearer exposures contain both unidirectional and bidirectional trough cross-stratification (Fig. 5C–G) in addition to planar stratification (Fig. 5E–H). Cross-beds range in thickness from 8 to 40 cm, with sets organized into co-sets that display no marked upward fining. Most beds have erosional and planar bottom and top contacts, though where true substrates (sensu Davies and Shillito 2019) have been preserved, both ripple marks (Fig. 6A–D) and adhesion marks (Fig. 6E, F) can be observed. Channel bases are sometimes marked by laterally discontinuous lags of angular mud clasts (Fig. 6G). Bed-parallel clasts of sandstone are also infrequently observed in planar-stratified sandstone beds (Fig. 6H). Sandstone beds internally display variously oriented depositional surfaces (Fig. 7A–D), with paleoflow relationships indicating that both lateral (bedform migration 60–120° relative to the underlying surface) and downstream (bedform migration ± 30° downslope of the underlying surface) modes of accretion are represented (see Long 2011; McMahon et al. 2017b). Many large accretion surfaces are only partially preserved, with topsets erosionally truncated by succeeding strata (Fig. 7D). Stratification succeeding more completely preserved accretion packages is typically flat laminated or has low-angle

slip faces (Fig. 7E). Accretion packages contain clasts up to 4 cm in diameter, the coarsest clasts observed anywhere in the studied Rawnsley Quartzite stratigraphy (Fig. 7F). Soft-sediment deformation affects a minority of beds and includes both small-scale foreset contortions and the deformation of entire stratigraphic horizons (Fig. 7G, H). Whilst recognizable channel forms have depths no greater than 5 m, packages of accreting stratification between a bottom and top erosional surface may be greater than 10 m thick (Fig. 7A).

Paleobiology.—No paleontological, ichnological, or microbial signatures were observed in Facies 1.

Interpretation.—The occurrence of cross-bedding indicates deposition from subaqueous dunes. Planar-stratification indicates critical or super-critical flow conditions at times of high discharge or reduced water depth (Fielding 2006; Cartigny et al. 2014). The channelized geometry and presence of bidirectional cross-stratification suggests tidal currents operating above effective wave base. Mud clasts lining the bases of Facies 1 deposits are interpreted to have been deposited on tidal erosion surfaces. Bed-parallel sandstone clasts, described in detail in Facies 5 (the facies in which they are most abundant), are the possible remnants of organically bound substrates ripped up and transported as cohesive intraclasts within a flow (e.g., Pflüger and Gresse 1996; Tarhan et al. 2017). Accretion deposits internal to individual sandstone packages are interpreted as the product of mobile migrating barforms. Most barform deposits have erosional upper contacts (Fig. 7D), though more completely preserved solitary cross-beds can transition upwards into low-angle cross-stratified and planar stratified strata (Fig. 7E), representing transitional-upper- and upper-flow-regime conditions active at reduced water depths towards bar-tops (e.g., Fielding 2006). The internal geometry of the barform deposits is consistent with both downstream (Fig. 7A, B) and lateral modes of accretion (Fig. 7C) (e.g., Miall 1996; Long 2011; McMahon et al. 2017b). Soft-sediment deformation structures occur at different scales and probably had distinct triggers. Deformation in individual cross-stratified sets likely formed by flow-induced shear. Deformed horizons which exceed the lateral extent of typical outcrops may have formed through: 1) groundwater movement (e.g., Owen et al. 2011) or 2) seismic activity (e.g., Davies et al. 2005) (for further discussion see Facies 4).

A previous submarine-flow interpretation for Facies 1 (Gehling 2000, his facies C) is inconsistent with: 1) observed primary sedimentary
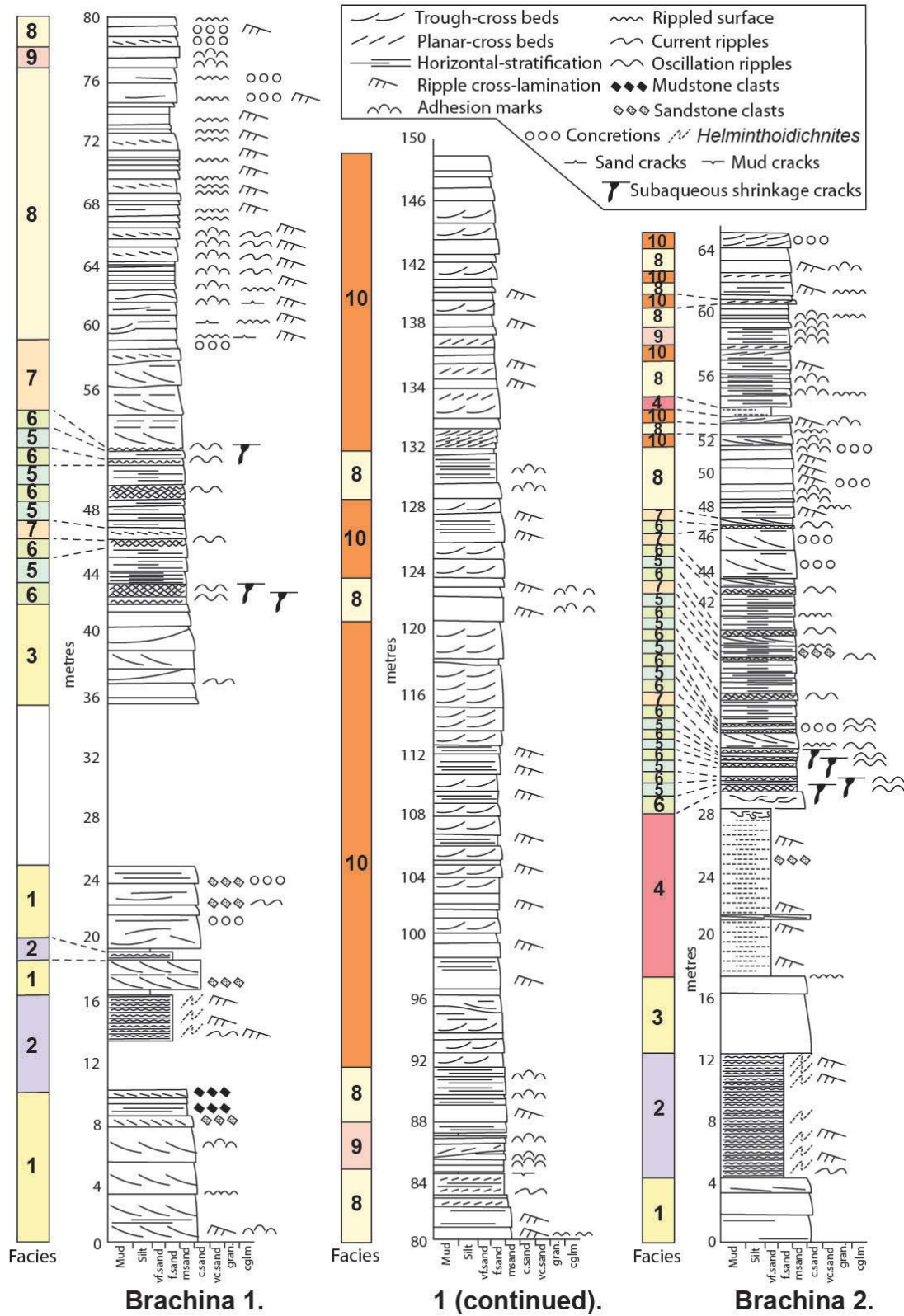
FIG. 3.—Detailed stratigraphic logs measured at Brachina Gorge. 1. Log base 31° 28′ 44″ S; 138° 33′ 40″ E. 2. Log base 31° 20′ 37″ S; 138° 34′ 12″ E.
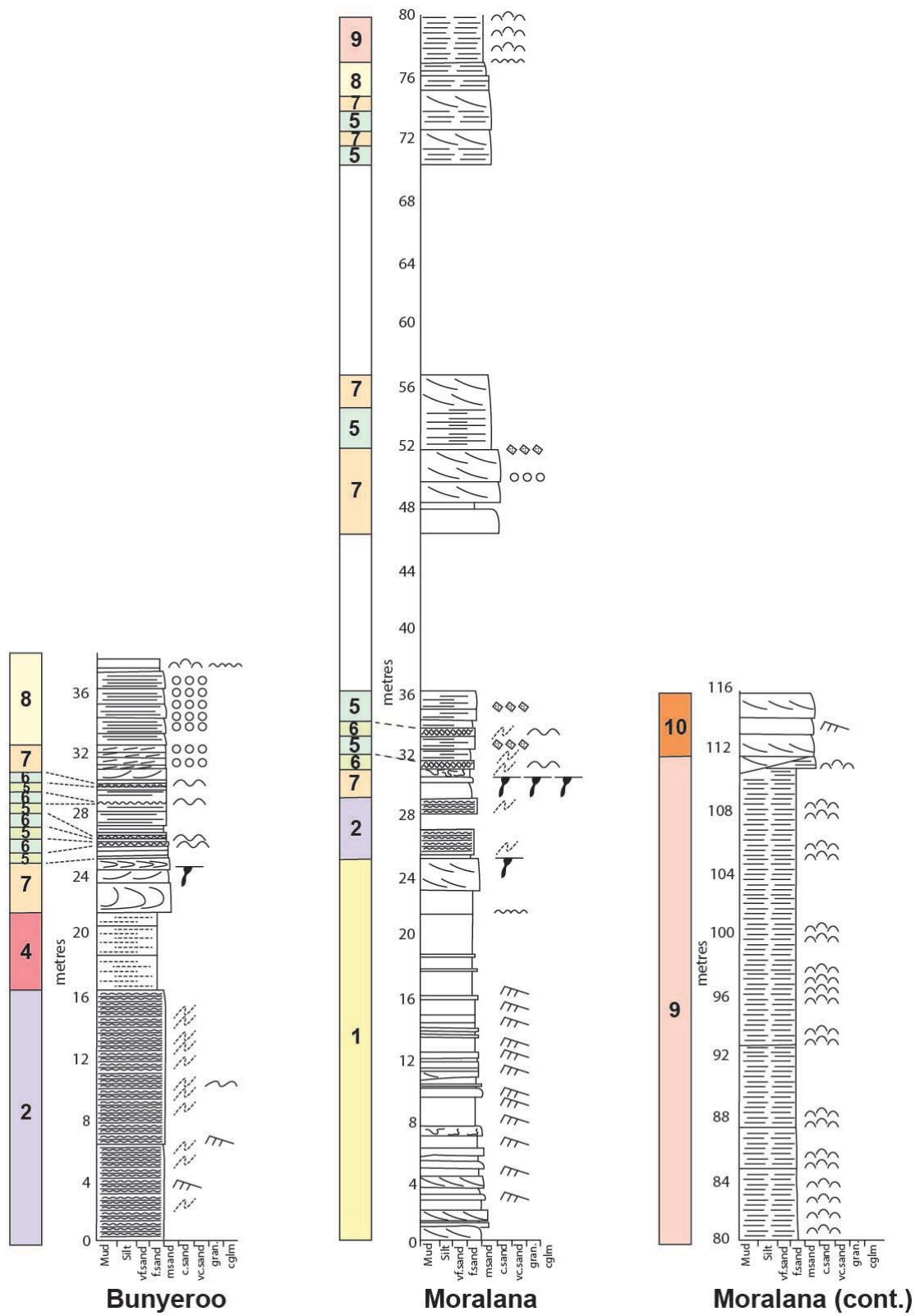
FIG. 4.—Detailed stratigraphic logs measured at Bunyeroo Gorge (Log base 31° 24′ 47″ S; 138° 32′ 30″ E) and Moralana (Log base 31° 32′ 19″ S; 138° 19′ 58″ E). See Figure 3 for key to symbols used.

TABLE 2.—*Characteristics of studied facies at Brachina Gorge, Bunyeroo Gorge, Moralana, and Wilpena Pound.*

Facies	Interpretation	Lithology	Sedimentary Structures/Fossils
1	Tidally influenced fluvial or estuarine (major) (Figs. 5–7)	Medium- to coarse-grained quartz-arenitic sandstone	Channel forms, trough-cross-stratification, bimodal stratification, planar stratification, ripple marks, adhesion marks
2	Mixed-flat (Figs. 8, 9)	Very fine- to fine-grained sandstone, siltstone, sandy mudstone	Flaser, wavy, and lenticular bedding, ripple cross-lamination, ripple marks, *Helminthoidichnites*, *Funisia* "buds"?
3	Tidally influenced fluvial or estuarine (minor) (Fig. 10)	Coarse-grained sandstone	Channel forms, planar stratification, ripple marks
4	Lagoon or interdistributary bay (Figs. 11, 12)	Siltstone to very fine-grained sandstone, rare medium-grained quartz-arenitic sandstone	Low-angle undulatory lamination, parallel lamination, low-angle cross-stratification, soft-sediment deformation, macrofossils, *Helminthoidichnites*
5	Lower shoreface (Fig. 13)	Medium-grained quartz arenitic sandstone	Planar stratification, macrofossils, *Helminthoidichnites*
6	Middle shoreface (Figs. 14, 15)	Fine- to medium-grained quartz-arenitic sandstone with siltstone drapes	Planar stratification, cross-stratification, oscillation ripple marks with interference patterns, current-ripple marks, subaqueous shrinkage cracks, macrofossils, *Helminthoidichnites*
7	Upper shoreface (Figs. 16, 17)	Medium-grained quartz-arenitic sandstone	Planar stratification, low-angle cross-stratification, planar- and trough-cross-stratification, poorly preserved *Aspidella*
8	Foreshore (Figs. 18–21)	Fine- to medium-grained quartz-feldspathic sandstone	Ripple-cross-lamination, planar stratification, low-angle cross-stratification, broad diversity of ripple marks (e.g., symmetrical, asymmetrical, ladder, rhomboid), adhesion marks
9	Backshore (Fig. 22A–F)	Fine- to medium-grained quartz arenitic sandstone	Adhesion ripples and marks, planar lamination
10	Distributary channels or sandy shoals (Fig. 22G, H)	Medium to coarse-grained quartz-arenitic sandstone	Planar and trough-cross-stratification, ripple-cross-lamination, planar stratification

structures in all studied sections (for example, bipolar current flow is characteristic of inshore tidal settings, and uncommon in offshore and shelf environments; Fig 5D) and 2) the stratigraphic occurrence of this facies at the base of an incised-valley fill. Valleys incised into underlying strata imply relative sea-level fluctuation. Intertidal environments represented by the underlying Chace Quartzite Member (Counts et al. 2016) undoubtedly became emergent and erosive following a drop in relative sea level, with subsequent degradation producing discrete incised valleys. Reestablishment of sedimentation following increased relative sea level would fill any available accommodation space. Our observations are consistent with an interpretation as tidally influenced fluvial or estuarine channels typical of such lowstand systems tracts, in which incised alluvial valleys are converted into estuaries by marine flooding (e.g., Allen and Posamentier 1994; Catuneanu 2006).

Facies 2. Ripple Cross-Laminated Heterolithic Sandstones

Sedimentology.—This facies comprises very fine- to fine-grained sandstones, siltstones, and rare sandy mudstones that exhibit flaser, wavy, and lenticular bedding (Fig. 8). Sandstone beds range in thickness from 2 to 10 cm. Ripple cross-lamination (Fig. 8C) and both symmetrical and asymmetrical rippled surfaces are present (Figs. 8A, B, D–F, 9A). Asymmetrical ripples have variable relief, with heights ranging from 0.5–3 cm. Lack of planform exposures mean that precise indications of ripple wavelength are unavailable. Mudstone clasts sometimes occur in sandstone beds (Fig. 9B). Interlaminated couplets of sand and silt provide reasonable evidence of rhythmic sedimentation (Fig. 9C). Thicker sandstone beds show evidence of sediment disruption towards bed tops (Fig. 9D), and evident scouring and subsequent infilling is regularly observed (Fig. 9E).

Paleobiology.—Meandering trace fossils assigned to *Helminthoidichnites* (e.g., Gehling and Droser 2018) present as surficial bilobed grooves or ridges on both bed tops and bases, and can be abundant on individual bedding planes (Fig. 9F). Traces are 1 to 3 mm wide, have distinct levees, and only rarely cross. Possible *Funisia* "buds" (circular bulbous bases to

Funisia organisms, e.g., Droser and Gehling 2008) were observed sporadically on rare bedding planes (Fig. 9G). Wrinkle marks, which have many potential microbial and abiotic origins (Davies et al. 2016), are rarely observed on siltstone bases (Fig. 9H).

Interpretation.—Alternations between sandstone and finer silts and muds demonstrate temporally variable current velocities. The resulting heterolithic facies may reflect either: 1) tidal influence or 2) interbedding of fair-weather and storm-generated beds. Considering that Facies 2 directly overlies tidally influenced Facies 1 strata (Figs. 3, 4), the former hypothesis is preferred. The high frequency of asymmetrical ripple forms and current-ripple cross-lamination demonstrates that sand was deposited largely as ripples migrating in response to subaqueous currents. Symmetrical ripples show that waves were responsible for the reworking of some substrates. Mud flasers may archive slack water conditions in between tidal cycles (de Raaf and Boersma 1971). Such tidal reworking would attest to deposition above the effective fair-weather wave base, a disconnect from much previous work, which considered this facies to have accumulated below maximum storm-wave base on the distal margins of prograding deltas (Gehling 2000; Gehling and Droser 2013; Tarhan et al. 2017). Moreover, linguoid ripples found in association with this facies at other sites (Tarhan et al. 2017) are produced at current velocities unlikely to occur in deeper-water settings (Reineck and Singh 2012).

An immediate transition from the demonstrably emergent Facies 1 (Fig. 6E, F) to the previously proposed sub-storm-wave base facies is considered improbable unless a separating stratigraphic hiatus of unknown duration exists. Without unambiguous evidence for emergence in Facies 2, an offshore environmental setting also remains possible (Fig. 2), since regions lying at or marginally seaward of the effective fair-weather wave base regularly accumulate distal tempestite (sand-rich) deposits interbedded with normal fair-weather strata (silts and muds) (e.g., MacEachern and Bann 2008). However, we argue that weighted evidence of sedimentary facies and stratigraphic context favor a low-energy tidal environment, potentially an intertidal mixed-flat or subtidal shoal. Such settings develop along gently dipping coastlines with marked tidal rhythms, with available
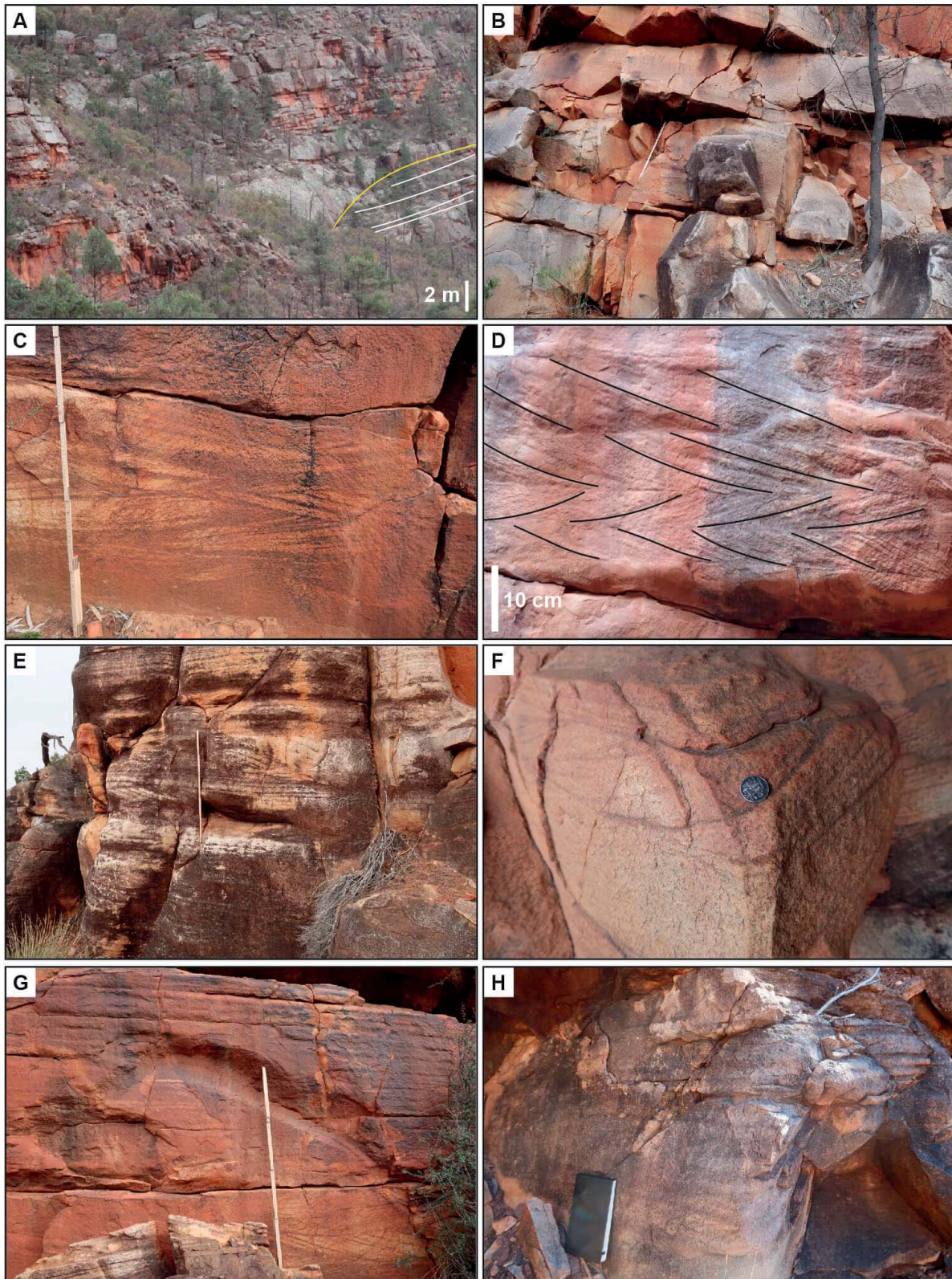
FIG. 5.—Sedimentary structures in Facies 1. **A)** Channel-form incision into underlying tabular sandstones. Wilpena Pound. **B)** Apparently massive, structureless sandstone. Lack of evident sedimentary structure is due to pronounced weathering. Brachina Gorge. **C)** Trough-cross-stratified sandstone. Wilpena Pound. **D)** Herringbone cross-stratification. Wilpena Pound. **E)** Cross-stratified and planar stratified sandstone. Wilpena Pound. **F)** Trough cross-stratification succeeded by planar stratification. Brachina Gorge. **G)** Trough cross-stratification succeeded by thick succession of planar stratification. Wilpena Pound. **H)** Planar stratification. Brachina Gorge. Coin diameter is 28.5 mm. Notebook is 20 cm long. Ruler is 1 meter long.
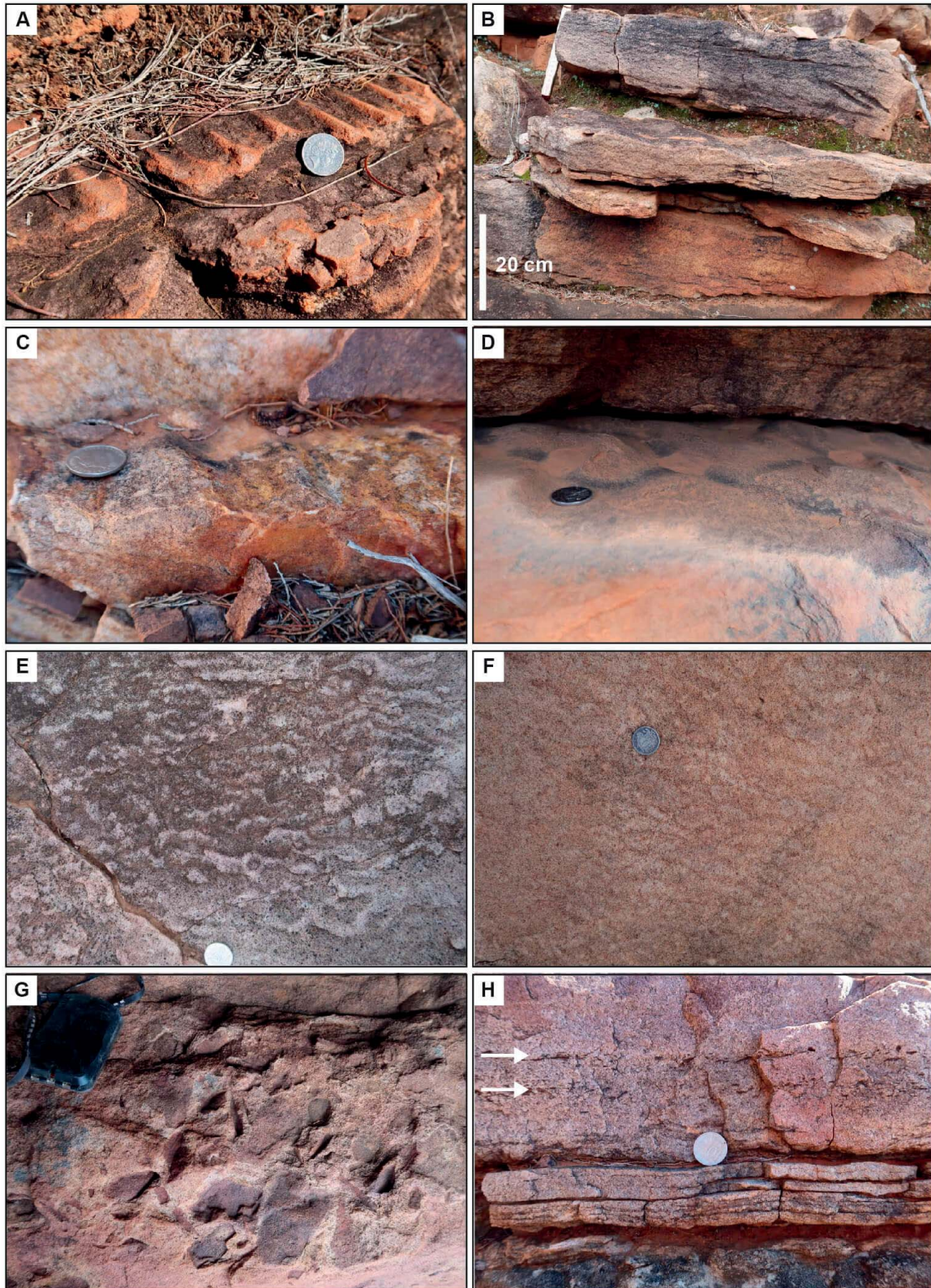
FIG. 6.—Sedimentary structures in Facies 1. **A)** Symmetrical ripple marks. Wilpena Pound. **B)** Ripple-cross-lamination. Brachina Gorge. **C)** Symmetrical ripple marks. Poor example is deliberately chosen to emphasize that many key sedimentary surface textures in this facies are poorly exposed. Brachina Gorge. **D)** Poorly preserved linguoid ripple marks. Wilpena Pound. **E)** Adhesion marks. Bunyeroo Gorge. **F)** Adhesion marks. Wilpena Pound. **G)** Intraformational mud clasts. Wilpena Pound. **H)** Bed-parallel sandstone clasts (white arrows). Brachina Gorge. Coin diameter is 28.5 mm. Compass is 10 cm long.
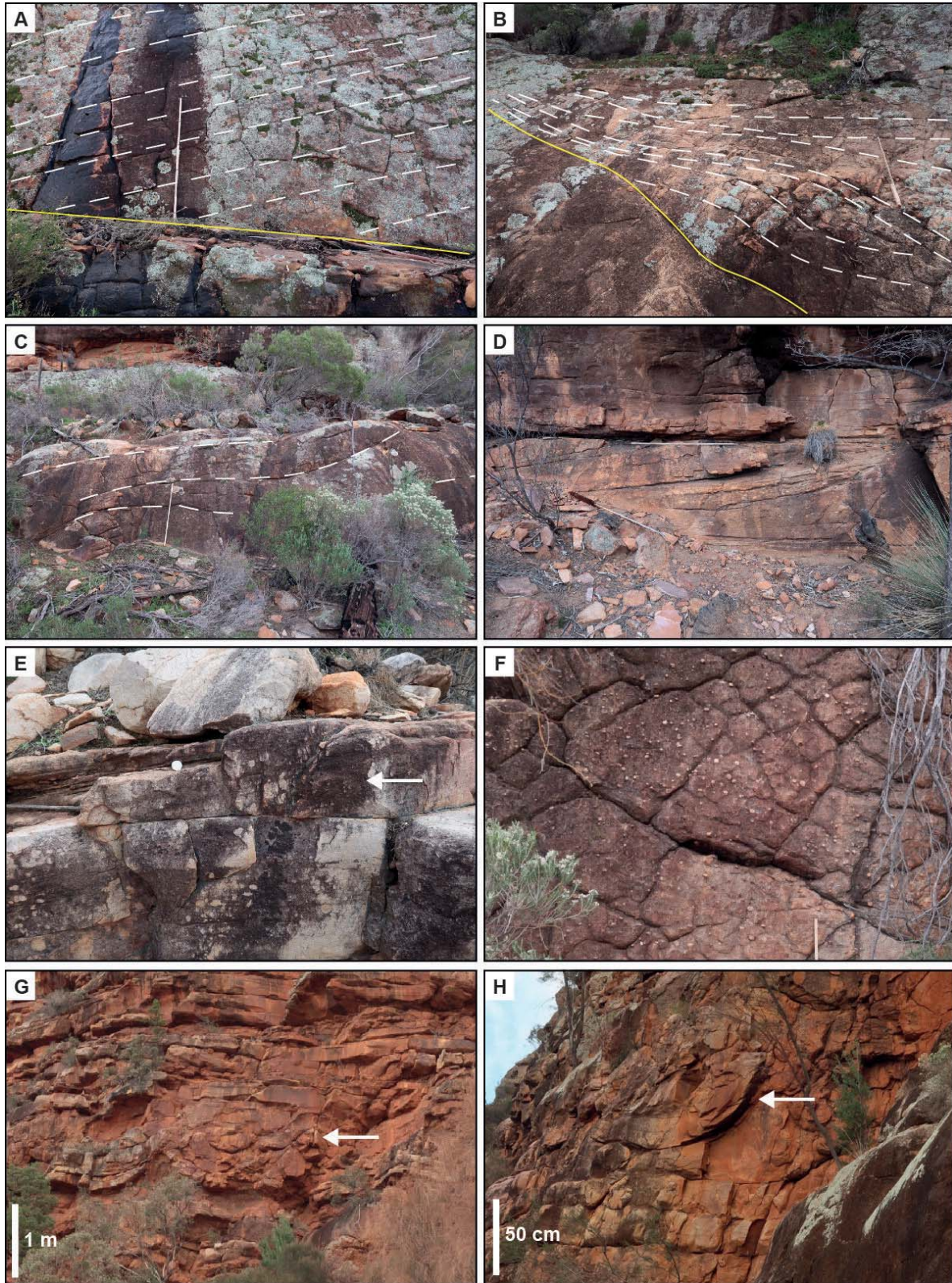
FIG. 7.—Sedimentary structures in Facies 1. **A)** Downstream-accreting barform. Wilpena Pound. **B)** Downstream-accreting barform with irregular slip faces. Wilpena Pound. **C)** Laterally accreting barform. Wilpena Pound. **D)** Barform slip faces top-truncated by succeeding strata. Wilpena Pound. **E)** Low-angle cross-stratification overriding barform deposit. Wilpena Pound. **F)** Granules and pebbles in sandstone matrix. Wilpena Pound. **G)** Laterally extensive horizon of deformed strata (white arrow). Wilpena Pound. **H)** Large-scale soft-sediment deformation (white arrow). Wilpena Pound. Coin diameter is 28.5 mm. Rule in Parts A–D and Part F is 1 meter long.
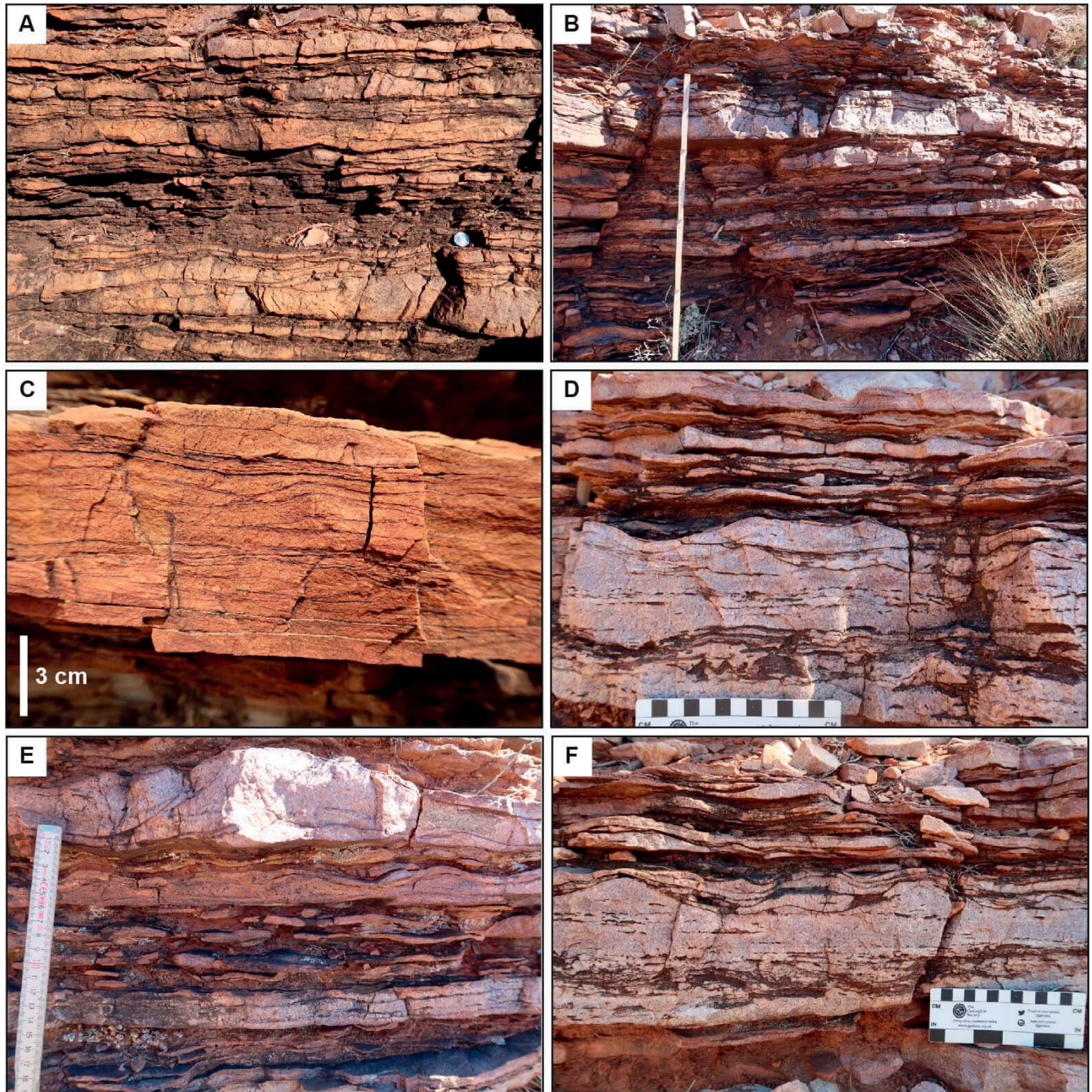
FIG. 8.—Sedimentary structures in Facies 2. **A, B)** Intercalated sandstone and siltstone displaying lenticular and flaser bedding in addition to asymmetrical ripples. Brachina Gorge. **C)** Ripple cross-lamination with flaser bedding. Bunyeroo Gorge. **D)** Lenticular bedding. Sandstone beds contain floating mud clasts. Brachina Gorge. **E, F)** Lenticular bedding with symmetrical and asymmetrical ripples. Brachina Gorge. Coin diameter is 28.5 mm. Rule in Part B is 1 meter long.

sediment but lacking significant wave action (Kleinhans et al. 2012, 2015). This could occur in estuaries, lagoons, bays, or behind barrier islands or other sand bars. Given that the Ediacara Member fills discrete incised valleys (Gehling 2000; Tarhan et al. 2015) and Facies 2 has a stratigraphic occurrence immediately overlying Facies 1 in the studied locations (Figs. 3, 4), we consider estuarine deposition to be most plausible. The absence of emergent, desiccated surfaces may in part be due to the apparent decreased abundance of preserved muddy terrestrial and paralic substrates before the

evolution of land plants (e.g., Bradley et al. 2018; McMahon and Davies 2018a), a hypothesis that requires further testing.

Facies 3. Amalgamated Channelized Sandstone

Sedimentology.—This thin facies was observed to crop out only at Brachina Gorge, where 3–6 m of coarse sandstone separates the underlying Facies 2 from the overlying Facies 4 (Fig. 10A). The sandstones are
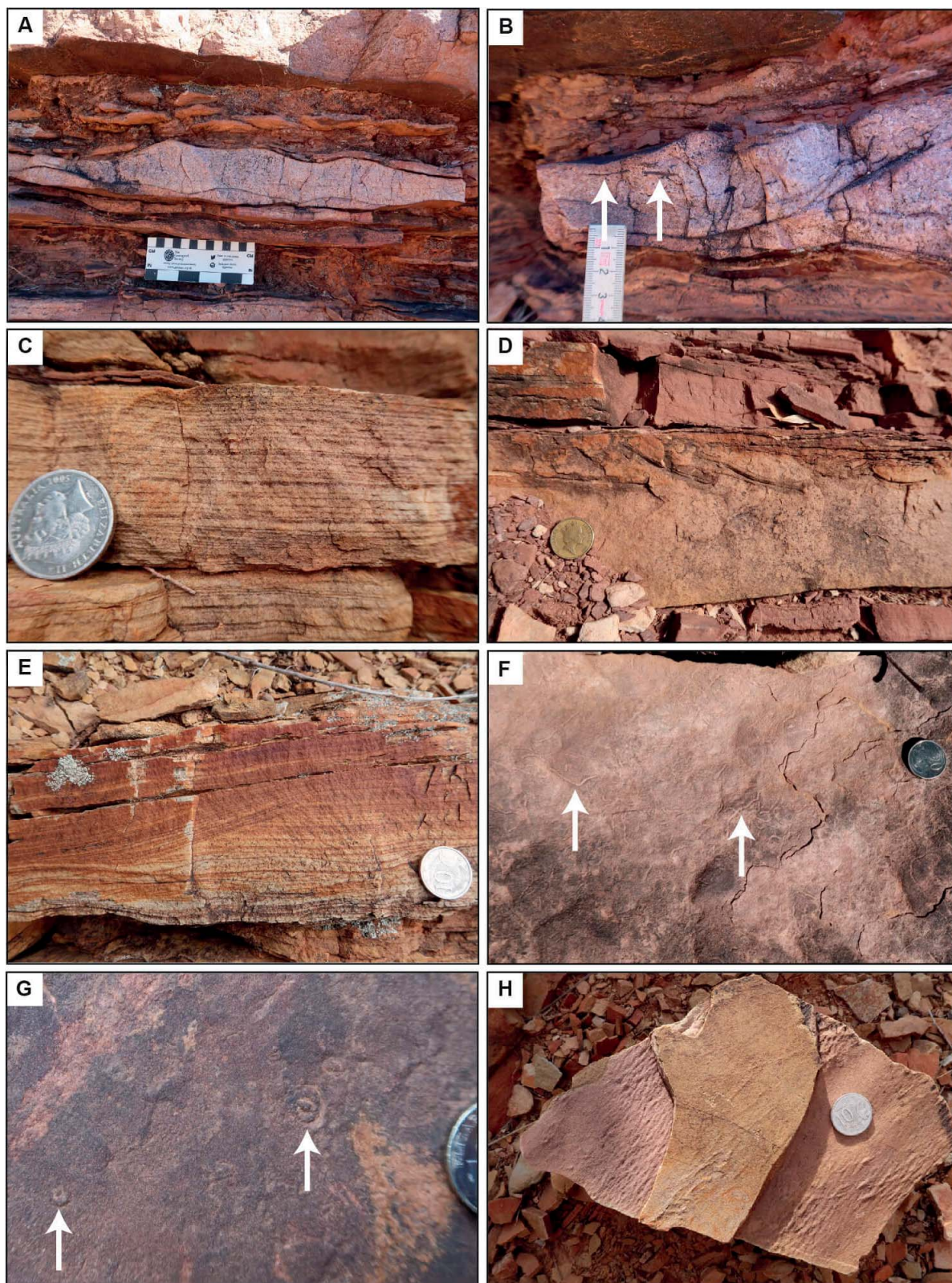
FIG. 9.—Sedimentary structures in Facies 2. **A)** Heterolithic asymmetrical ripples in lenticular-bedded strata. Wilpena Pound. **B)** Sandstone veneer with mud clasts (white arrows) flanking asymmetrical rippled surface. Brachina Gorge. **C)** Interlaminated couplets of sand and silt. Bunyeroo Gorge. **D)** Evident sediment disruption towards the top of a sandstone bed. Bunyeroo Gorge. **E)** Filled scour margin. Bunyeroo Gorge. **F)** Meandering trace fossils assigned as *Helminthoidichnites* (arrowed). Brachina Gorge. **G)** Circular impressions resembling *Funisia* "buds" (bases) (arrowed). Brachina Gorge. **H)** Transverse wrinkle marks. Brachina Gorge. Coin diameter is 28.5 mm.
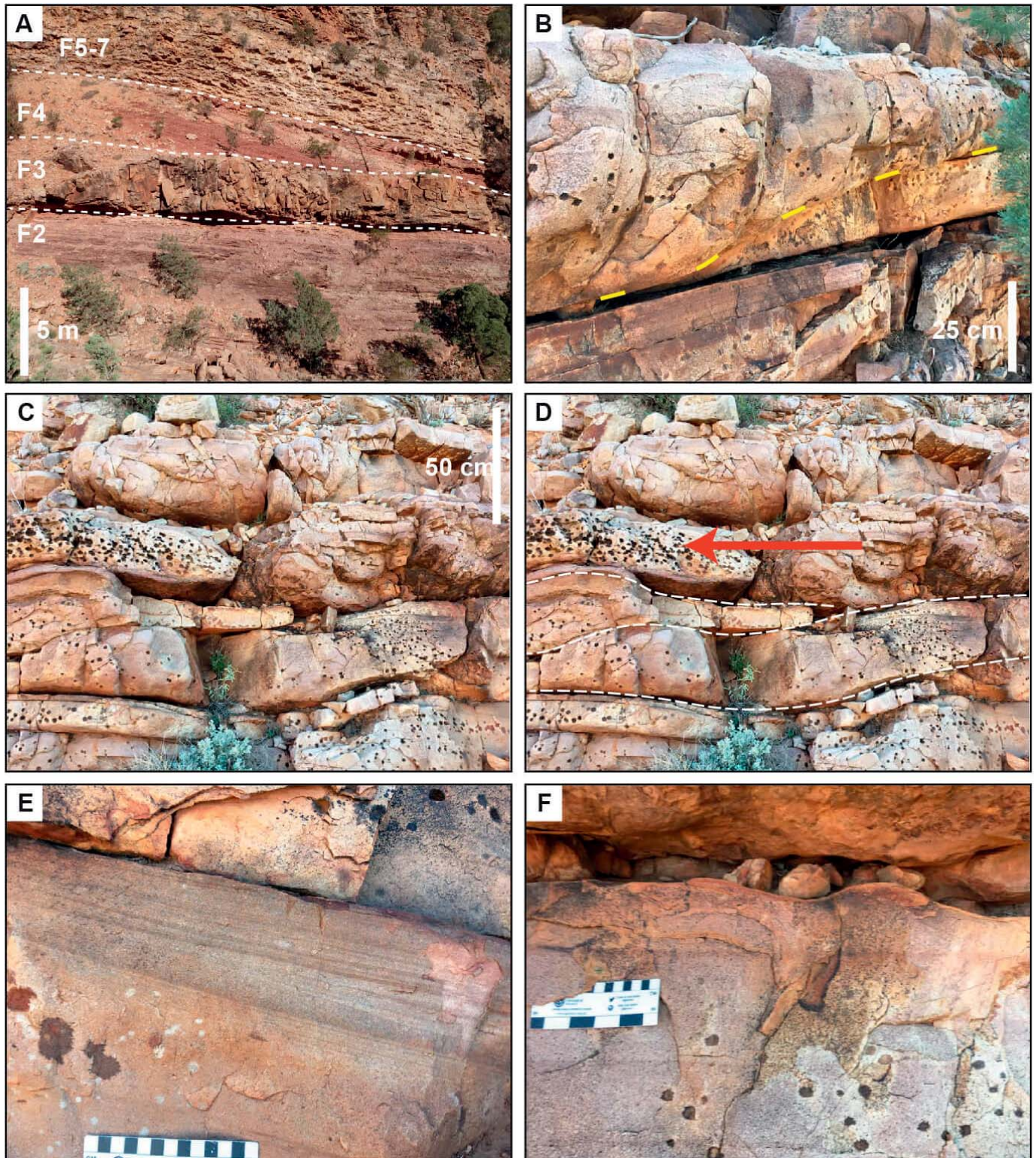
FIG. 10.—Sedimentary structures in Facies 3. **A)** Stratigraphic context of Facies 3 at Brachina Gorge. See Figure 2 for detailed sedimentary log. **B)** Minor channelized form in a sandstone body. **C)** Lateral-accretion elements. **D)** Line-drawing over Part C, picking out lateral-accretion sets. Red arrow shows the direction of accretion. **E)** Planar stratification. **F)** Ripple-marks. Note nodule pseudomorphs beneath scale bar. All photographs Brachina Gorge.

typified by multiple erosional surfaces, which depict both channelized (Fig. 10B) and lateral-accretion elements (Fig. 10C, D). One channel element can be recognized in its entirety, measuring 70 cm deep and 23 m wide, with evident lateral-accretion surfaces flanking one channel margin (Fig. 10C). Planar-stratification is the dominant internal sedimentary structure (Fig. 10E), with ripple marks recognizable on some bed tops (Fig. 10F).

This facies differs from Facies 1 in lacking cross-stratification of any kind, having distinct lateral-accretion surfaces that result in far less tabular beds, and comprising individual channels no greater than 1 m in depth (as opposed to upwards of 5 m in Facies 1).

Paleobiology.—No paleontological, ichnological, or microbial signatures were observed in Facies 3.

Interpretation.—Facies 3 is interpreted as the active fill of laterally migrating, possibly estuarine channels. The relatively small dimensions of individual channel-forms, relatively insignificant thickness of the facies as a whole, and occurrence only in local sections suggests that these were minor, spatially discontinuous conduits. Their far smaller dimensions, distinct sedimentary structures, evident lateral accretion and association with the overlying Facies 4 lead us to separate Facies 3 from Facies 1. Laterally accreting barforms can act as a proxy for original water depth (e.g., van der Lageweg et al. 2016), with specific examples here (Fig. 10D) demonstrating that at times during Facies 3 deposition water depth was little more than 50 cm.

Facies 4: Red Silty Sandstone

Sedimentology.—This facies is dominated by maroon-colored beds of siltstone to very fine sandstone (Fig. 11). Primary sedimentary structures are generally limited to thin (1 to 4 mm), low-angle undulatory, parallel-laminated beds in addition to rarer ripple cross-lamination (Fig. 11A–C). Individual layers are usually planar, though slight inclinations are occasionally apparent, potentially due to deposition on originally inclined surfaces (Fig. 11D). Convex-up laminae with distinct aggradational bed contacts are recognized in certain instances (Fig. 11E). Eroded hollows were observed on a singular occasion and indicate the former presence of intraformational clasts (Fig. 11F). No evidence of subaerial exposure was observed. Beds of low-angle cross-stratified medium-grained quartz arenites of 2 to 10 cm thickness occasionally punctuate the red siltstones (Fig. 11G). At Bunyeroo Gorge a distinct color change, from maroon to purple, exists towards the top of the facies (Fig. 11H).

When overlain by sandstones of Facies 5 and Facies 6, the red siltstones are frequently loaded and display ball-and-pillow structures, with quartz-arenitic sandstone layers typically dissected into numerous distinct ellipsoidal bodies (Fig. 12A). These pillows are either connected to the overlying quartz-arenitic coarse sandstone (Fig. 12A), or are floating in the red siltstone matrix (Fig. 12B). The pillows themselves contain deformed, curved laminae (Fig. 12B). Soft-sediment-deformed strata include one laterally discontinuous "lens" of coarse-grained quartz-arenitic sandstone (Fig. 12C). This sole example shows deformed bedding planes with vertical dimensions of nearly 4 m. The primary cross-stratified surfaces in this deformed bed remain preserved (Fig. 12D). In the red siltstones themselves, soft-sediment deformation is restricted to lamina-scale mildly disrupted bedding (Fig. 12E).

Despite a different dominant grain size and markedly distinct internal sedimentary structures (see also Facies 2 Description), Facies 4 has been grouped with Facies 2 in past studies (e.g., Facies E of Gehling 2000; and the "current ripple sand facies" of Reid et al. 2020). The last work to treat this facies individually was by Jenkins and colleagues (Jenkins et al. 1983, their Facies A). The unit is thickest at Mayo Gorge (reportedly 53 m; Jenkins et al. 1983), but at the studied sites ranges from 11.1 m at Brachina

Gorge to absent at Moralana. At Brachina Gorge, faults repeat the entire Ediacara Member section (Gehling 2000). Facies 4 is absent from one of these two faulted sections (Fig. 3), emphasizing the unit's variable thickness even over short distances. Given the transitional relationship between the red siltstone facies and the relatively undeformed overlying quartz-rich sandstone facies (Facies 5 and 6; Fig. 12A), in this study we consider soft-sediment-deformed strata as a discrete characteristic of Facies 4 rather than a separate facies (whilst recognizing that this grouping is not ideal: for example, soft-sediment-deformed strata occupy a similar stratigraphic position between underlying Facies 2 and overlying Facies 5 strata in sections at Moralana where Facies 4 is absent (Fig. 12G)).

Paleobiology.—Macrofossils, microbial surface textures, and ichnofossils (*Helminthoidichnites*) occur in this facies, as both hyporelief and epirelief impressions (Reid et al. 2018).

Interpretation.—Lack of architectural context, homolithic character, and cryptic primary sedimentary structures make Facies 4 challenging to assign to a particular depositional environment. Laminar bedding and overall finer grain sizes (though distinctly lacking in mudstone) imply deposition in tranquil water. Past observations of starved ripples imply minimal sand input (Jenkins et al. 1983). Coarse interbeds of transitional-upper-flow-regime structures (low-angle cross-stratification) suggest event-style splays most likely with a proximal source. The hinterland of a feeder system may contain a range of lithologies (Kleinhans 2010), and transport processes operating over sufficient length scales destroy labile minerals and sort sediment by grain size (Frings 2008). The siltstone component of this facies is unlikely to have been selectively sorted from other observed proximal siltstones (e.g., those in the flaser beds of Facies 2), suggesting that Facies 4 had a distinct proximal source with a differing lithology that could supply sufficiently thick layers of silt.

Based on comparison with modern examples, a lagoonal depositional environment was suggested by Jenkins et al. (1983). Pronounced thickness variation in this facies across the region, and its absence in some locations, demonstrates an environment with patchy spatial distribution, making a lagoon, as opposed to offshore or shelf environments, a plausible depositional setting. Observed coarse interbeds (Fig. 11G) may have formed as sand was brought into the lagoon during storm events, potentially as washover fans. Wave activity significant enough to form protective sand bars or barriers is evident in other facies (e.g., Facies 6), but the lack of evidence for such barrier environments preserved in Ediacara Member strata presents difficulties for this model. However, the spatial development, composition, and internal features of the observed deposits resemble some ancient lagoonal environments interpreted elsewhere (e.g., Tanoli and Pickerill 1990). Most other researchers have proposed that the siltstones accumulated below maximum (storm) wave base, either as a pelagic fall-out of fine sediment winnowed from delta sheets (Gehling 2000; Reid et al. 2020), or through rapid deposition in a delta-front to prodelta setting (Tarhan et al. 2017; Droser et al. 2019). Recumbent foresets present in one layer closely overlying Facies 4 (occurring as an interbed with the deposits of Facies 5 and 6) are similar to those observed in modern distributary channels that may feed delta-front environments (Fig. 12H). Regardless, the necessary base-level change from the underlying shallow-water (sub-meter) Facies 3 (Fig. 10) or, in one instance, cross-bedded Facies 10 (Fig. 11C), to the proposed sub-storm-wave-base deltaic setting (e.g., Gehling and Droser 2013; Tarhan et al. 2017) is considered unlikely. It does remain possible that a previously unrecognized hiatus exists in some individual Ediacara Member sections, which could account for some of the observed stratigraphic discontinuities. Until more evidence is uncovered, in this study we consider the deposits of Facies 4 to have formed in a lagoon or an interdistributary bay interjected by washover fans. However, we emphasize that this interpretation is informed by consideration of the relative stratigraphic position of the facies
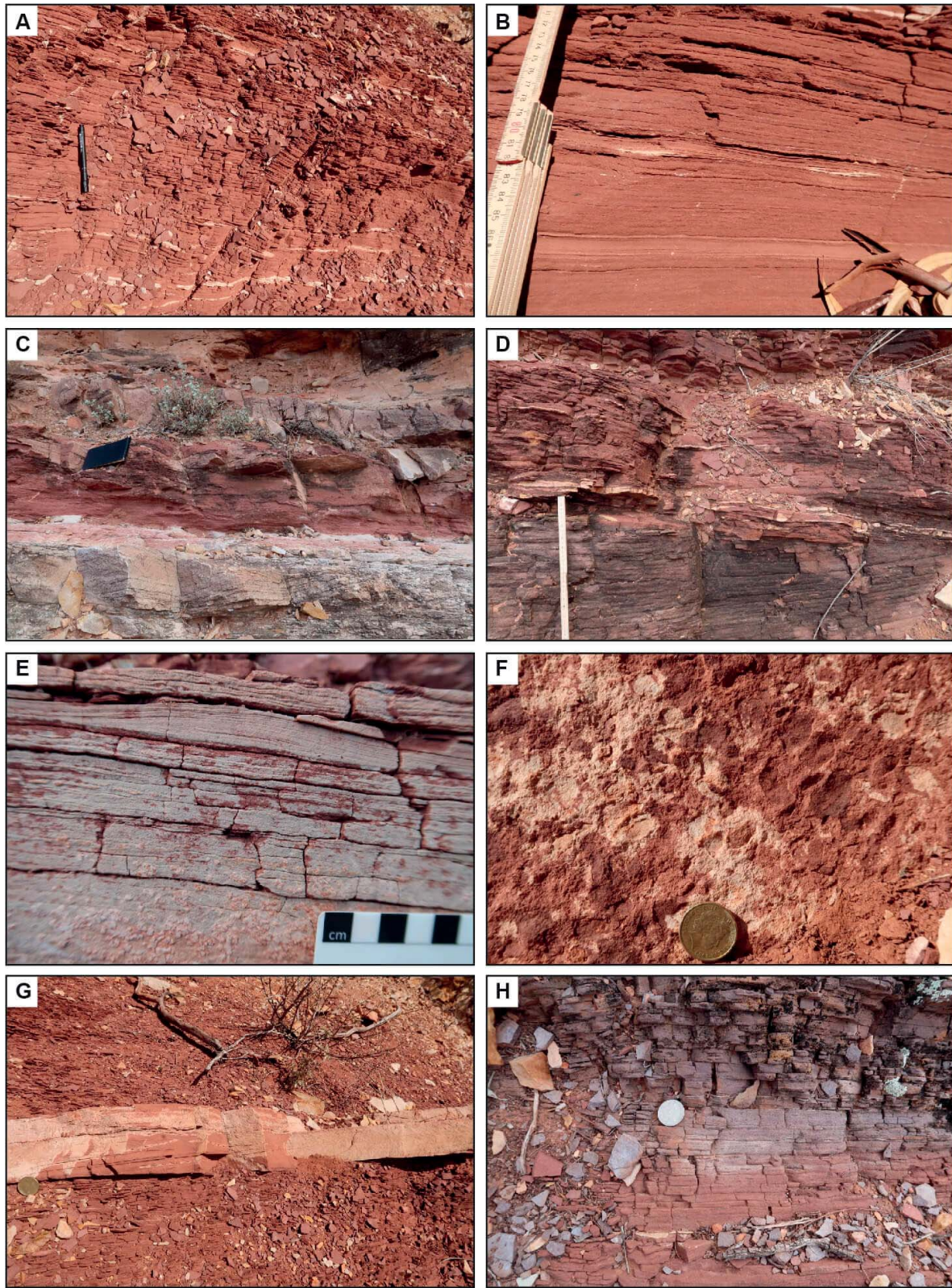
Fig. 11.—Sedimentary structures in Facies 4. **A**, **B)** Parallel-laminated red siltstone. Brachina Gorge. **C)** Red siltstone directly overlying minor channel with cross-stratified fill (Facies 10). Brachina Gorge. **D)** Vertically juxtaposed siltstones with different degrees of tilt. Bunyeroo Gorge. **E)** Convex-up-laminae with aggradational contacts. Bunyeroo Gorge. **F)** Eroded molds of intraformational clasts. Brachina Gorge. **G)** Quartz-arenitic low-angle cross-stratified sandstone punctuating red siltstone deposit. Brachina Gorge. **H)** Maroon to purple color change at Bunyeroo Gorge. Pen is 14 cm long. Notebook is 20 cm long. Coin diameter is 28.5 mm. Rule showing in Part D is 40 cm long.
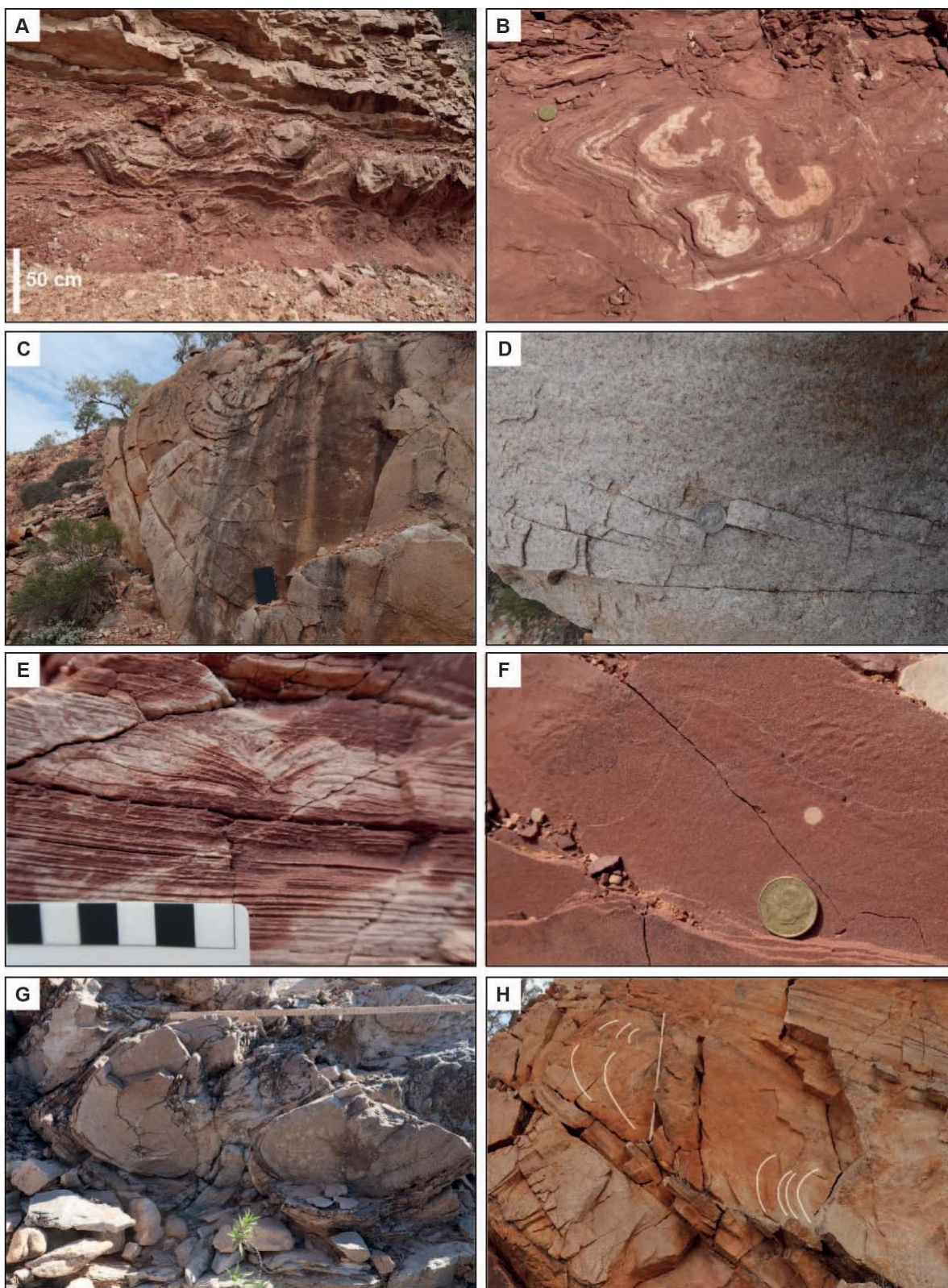
Fɪɢ. 12.—Sedimentary structures in Facies 4. **A, B)** Ball-and-pillow structures. Brachina Gorge. **C)** Large-scale soft-sediment deformation at Bunyeroo Gorge. **D)** Preserved primary cross-stratification in Part C deformed beds. **E)** Minor sediment disruption. Bunyeroo Gorge. **F)** Bulbous loading structures. Bunyeroo Gorge. **G)** Ball-and-pillow structures. Moralana. **H)** Recumbent foresets. Bunyeroo Gorge. Notebook is 20 cm long. Coin diameter is 28.5 mm. Rule for scale in Parts G and H is 1 meter long.

with respect to the underlying (Facies 3) and overlying (Facies 5–7) strata (Figs. 3, 4), and alternative origins for the Facies 4 silty sandstones remain possible (Gehling 2000; Retallack 2012; Gehling and Droser 2013; Tarhan et al. 2017; Reid et al. 2020).

Deformed horizons associated with Facies 4 (Fig. 12A–C, G) have been considered as forming both *in situ* with no lateral movement (Jenkins et al. 1983 (through discussion with Mary Wade, p. 109)) or as slumped, mass flows or sediment gravity flows cascading into submerged canyons (Gehling 2000; Gehling and Droser 2013; Tarhan et al. 2015, 2017; Reid et al. 2020). A submarine-canyon interpretation does not adequately account for the rapid base-level fluctuations required to account for stratigraphic sandwiching of this facies between shallow-water, channelized strata (Facies 3, Facies 10) and overlying shoreface sands (Facies 5, 6). The premise that rapid deposition of unstable sediment piles as slump deposits would be dependent on an associated steep landward slope (Gehling 2000), is not the only possible solution. Sudden liquefaction of large masses of sand is also a common phenomenon after bank failure in estuaries and rivers (Van den Berg et al. 2002), with deposits manifesting in stratigraphy as similar convolute lamination and ball-and-pillow structures (Lowe and Guy 2000).

Importantly for the Ediacara Member examples, the preservation of primary (subcritical) sedimentary structures in deformed beds (Fig. 12D) favors *in situ* deformation, since transportation as water-saturated (fluidized) flows would be expected to cause complete sediment reworking and resultant destruction of primary bedforms (Postma et al. 1983). Lateral continuity of deformed horizons across individual outcrops, and the close correlation of deformed horizons between studied successions raise the possibility that deformation may have been the product of a single seismic event (e.g., Davies et al. 2005). Variable expressions of soft-sediment-deformed structures (ball-and-pillow structures, upturned beds, convolute cross-stratification) would then result from variations in sedimentary facies at the time of seismic shock. Many examples of soft-sediment deformation are attributed to seismic activity, but evidence is often variable and inconclusive (Owen et al. 2011). Work is ongoing to conclusively identify a causal mechanism for the Ediacara Member deformed beds, and to confirm the original depositional environment for this facies as a whole.

Facies 5. Planar Stratified Sandstones with Fossil Taxa

Sedimentology.—Quartz-rich medium-grained sandstones with planar erosional bases and containing ungraded sets of planar stratification dominate this facies (Fig. 13A). The thickness of individual deposits ranges from a few centimeters to 2.1 m (Fig. 13B). Locally, inclined stratification is developed amongst predominantly planar stratified slip faces (Fig. 13C). Successions are usually erosionally amalgamated (Fig. 13D), but where succession tops are preserved, subtle reworking by combined-flow ripples can be apparent. Rip-up clasts of sandstone are most abundant in this facies (Fig. 13E; these are also present in Facies 1 and 8). Described in detail by Tarhan et al. (2017), sandstone clasts are most often flat and either ellipsoidal or irregularly shaped. Often clasts have rounded edges and range from 0.5 to 5.0 cm in maximum dimension.

Paleobiology.—Trace fossils (in the form of *Helminthoidichnites*) and body fossils (Fig. 13G) are commonly found in this facies, predominantly as hyporelief impressions (e.g., Droser et al. 2019), but with some epirelief preservation. Discrete microbially induced sedimentary surface textures (without associated macrobiota) were not observed, although sandstone clasts archive potential evidence for the former presence of microbial mats. Deposition as individual clasts indicates a pliant response of the sand clasts to flow, suggesting the need for a cohesive (elastic) binding agent (Pflüger and Gresse 1996). Given the high abundance of microbial-surface textures in the associated Facies 6, a covering microbial mat seems a plausible candidate for this binding agent (Tarhan et al. 2017). Storms presumably

were responsible for the erosion of landward-directed, mat-covered sand layers, and their subsequent deposition as intraclasts in this facies. Rip-up clasts of sandstone are not entirely anactualistic Precambrian sedimentary phenomena (*contra* Tarhan et al. 2017), and are known from some Phanerozoic strata (Menzies 1990; MacNaughton et al. 2019; Sarkar and Banerjee 2020).

Interpretation.—Monotonous grain size and paucity of internal erosional surfaces indicate that each Facies 5 succession was deposited by an individual event. Deposition had been previously considered to have occurred as "sheet flows" in submarine canyons beneath the storm wave base (Gehling and Droser 2013; Droser and Gehling 2015). No mechanistic explanation for how "sheet flows" in submarine canyons operate has been given (or explanation of how "sheet flows" differ from the distinct "mass flows" also interpreted to have occurred in submarine canyons (e.g., Gehling and Droser 2013, their Figure 1)). Sheet flow is a non-specific term, more widely used for the description of terrestrial, low-magnitude and high-frequency unchannelized flows (North and Davidson 2012), and for stratification formed in high sediment mobility under nearshore wave conditions (Passchier and Kleinhans 2005; Quin 2011). It is recommended that use of the term be discontinued in the context of the Rawnsley Quartzite.

We contend that deposition of Facies 5 more likely occurred on the lower shoreface during high-energy events, most probably storms. The lower shoreface begins at the lower limit of the fair-weather wave-base and extends landward to the zone where shoaling and initial breaking of waves is more prevalent (Reinson 1984) (Fig. 2). In many extant systems, ubiquitous sandstone deposits are confined to the upper shoreface and foreshore (see Stratigraphic Organization) (e.g., Reineck and Singh 2012). During storms, sand is eroded from these areas and transported basinward in suspension by turbulent water. Deposition of remobilized sand predominantly occurs in the lower-shoreface region, typically forming planar stratified or low-angle cross-stratified deposits. Such deposits are well reported from both modern (Hill et al. 2003; Clifton et al. 2006) and ancient (Arnott 1993; Went 2013) lower-shoreface environments.

As single-event beds, the taphonomic and ecological implications for reducing hypothesized water depths from the previously envisioned submarine canyon fills (e.g., Gehling and Droser 2013; Tarhan et al. 2017) to the lower-shoreface are minimal. Planar stratification is a consequence of high-energy, combined flow (flow with both unidirectional and oscillatory components) (e.g., Arnott 1993). Deposition during storm events would result in burial (and possible transportation) of fair-weather benthic communities as previously proposed (Droser and Gehling 2015) (Fig. 13G, H). Fast burial would also protect the succession from subsequent reworking by waning waves, hence the scarcity of preserved combined-flow ripples. Rarity of surfaces representing periods of sedimentary stasis also accounts for the paucity of associated microbially induced sedimentary surface textures. The topmost package of an individual set, where such ripple marks might be expected (e.g., Arnott 1993) is most often erosively top-truncated by the succeeding deposit. Intervals without significant erosional amalgamation or top truncation may record waning-stage oscillation or combined-flow-ripple lamination capping planar-stratified beds, but most often these facies are restricted to shallower middle-shoreface settings (Facies 6).

It is crucial to exercise caution when inferring Ediacaran habitats from this facies, since examples of equifinality (the possibility that multiple different processes could result in similar end products; Davies et al. 2020) are widespread. For example, planar stratified sands do not necessarily imply nearshore marine sedimentation, with such deposits also typical of critical-flow conditions or ephemeral swash conditions in the littoral zone and on land. Meanwhile, sandstone rip-up clasts have been recognized in emergent foreshore facies (Fig. 13F) (sand-flat facies in Gehling 2000),

Fig. 13.—Sedimentary structures in Facies 5 (apart from Part F). **A**, **B)** Planar stratification at **A)** Brachina Gorge and **B)** Moralana. **C)** Inclined stratification with erosional base downcutting into underlying planar stratification. Brachina Gorge. **D)** Multiple sets of planar stratification separated by erosional discontinuities. **E)** Sandstone rip-up clasts. Moralana. **F)** Adhesion marks overlying planar stratified sandstones with intraformational sand clasts (arrowed). Bunyeroo Gorge (Foreshore facies, Facies 8). **G)** *Dickinsonia* on the sole surface of loose block shown in Part H, from Moralana. Burial by low-angle cross-stratified sandstone demonstrates shallower water depths than previously proposed sub-storm-wave base "sheetflow" environments (e.g., Gehling and Droser 2013). Notebook is 20 cm long. Coin diameter is 28.5 mm. Rule shown in Part A is 14 centimeters long. Rule for scale in Part B is 1 meter long.

estuarine channels (Facies 1, Fig. 6G), and lower-shoreface deposits (Fig. 13E).

Facies 6: Oscillation-Ripple Facies

Sedimentology.—This facies comprises fine- to medium-grained quartz arenitic sandstones and millimeter-thick draping siltstone and very fine sandstone interbeds (Fig. 14A–E). Sandstone beds are generally erosionally amalgamated, < 1 to 30 cm thick, and rarely greater than 10 m in lateral extent. Internally, beds may contain a single set of unidirectional cross-strata (Fig. 14F), but more commonly display planar stratification (Fig. 14E). Bed tops show evidence of reworking by oscillation vortices such that bedding planes dominantly comprise oscillation-ripple marks (height, 2 to 5 cm; wavelength 3 to 14 cm). Ripple marks are discontinuous and show frequent bifurcation and discordant interference patterns (Fig. 15A, B). Straight unidirectional-current-rippled bed tops are subordinate (though present at every studied location; Fig. 15C). Subaqueous shrinkage cracks (previously referred to as synaeresis cracks; Gehling 2000; Reid et al. 2020) are widespread (Fig. 15D–F). Whilst most sandstone beds are separated by a millimeter-veneer of siltstone or fine sandstone (Fig. 14A–E), some juxtaposed rippled beds are entirely free of fine particles (Tarhan et al. 2017). Hummocky cross-stratification has been figured in a single instance (Gehling 2000, his Fig. 10D).

Paleobiology.—If this facies directly correlates with the oscillation-rippled sandstones of previous workers (e.g., Tarhan et al. 2017; Reid et al. 2020), macrofossil assemblages in this facies include some of the most abundant, diverse, and most widely studied paleocommunities in the Ediacara Member, with at least 27 genera formally reported (Gehling and Droser 2013; Droser and Gehling 2015; Reid et al. 2018; Droser et al. 2019; Evans et al. 2019). In contrast to the macrobiota, the trace-fossil suite in the sandstone beds is of low diversity, although *Helminthoidichnites* can be common on the bases of thin sandstone beds (Gehling and Droser 2018). Microbially induced sedimentary surface textures (referred to as "TOS" in previous works; e.g., Gehling and Droser 2009) are a common feature of Facies 6 bedding planes, with a patterned assemblage of fine reticulate ridges widely termed "elephant-skin texture" (Fig. 15G) being the most abundant. Also present are patchy clusters of dimple marks (Fig. 15H) described as "pucker" (Gehling and Droser 2009). The observed shrinkage cracks have been interpreted elsewhere to indicate salinity change (e.g., Carroll and Wartes 2003; Buatois et al. 2011), but recent work has demonstrated that biostabilization induced by microbial mats at the sediment–water interface may restrict pore-water movement sufficiently such that post-burial shrinkage can be accommodated by cracking (Harazim et al. 2013; McMahon et al. 2017a). Given the close association between microbial surface textures and subaqueous shrinkage cracks in Facies 6 (Fig. 15D–H), a microbial mechanism seems most likely. However, since the deposit is part of an incised-valley fill, and is closely associated with mixed-source estuarine deposits, salinity fluctuations cannot be entirely discounted as a mechanism of crack formation.

Interpretation.—Significant oscillatory wave energy and a preserved depositional record dominated by storm event beds is consistent with deposition on the middle shoreface (e.g., Walker and Plint 1992; Reineck and Singh 2012). The middle shoreface, above effective (fair-weather) wave base, extends over the zone of shoaling and initial breaking of waves (Reinson 1984) (Fig. 2). Storms have far greater influence on the middle shoreface than in any other shoreface environment, and storm deposits therefore constitute the greater part of the succession thickness (e.g., Fairchild and Herrington 1989; Dashtgard et al. 2012; Baniak et al. 2014). Thin, draped siltstones most likely settled from suspension or were deposited by more tranquil currents during periods of subdued (fair)

weather. Symmetrically rippled beds record episodes of minimal sediment supply, allowing winnowing of sediment by waves, the growth of microbial mats, and habitation by Ediacaran macrobiota. Interference patterns on *Aspidella*-bearing surfaces (Fig. 15B) strongly suggest shallow, littoral-zone sedimentation.

Facies 6 previously has been suggested to be situated in offshore environments between maximum (storm) and effective (fair-weather) wave base (Gehling 2000; Gehling and Droser 2013; Tarhan et al. 2017) (though see Reid et al. 2020, who suggested deposition in an upper fair-weather wave-base environment). Similar to the shoreface complex, offshore sediments also accumulate during both fair-weather and storm conditions. In contrast, the preserved depositional record of offshore complexes sees a predominance of fair-weather beds, with storm deposits constituting a regular, but subordinate, component of the succession (e.g., Dashtgard et al. 2012). Intercalation with overlying deposits consistent with upper-shoreface and foreshore deposition (Facies 7 and 8) makes a middle-shoreface environment more plausible than deposition beneath effective (fair-weather) wave base. Flattened unidirectional ripples (Fig. 15C) are also far more consistent with deposition above fair-weather wave base (e.g., Reineck and Singh 2012). One figured example of hummocky cross-stratification (Gehling 2000, his Fig. 10D) fits well in this revised evaluation: storms constitute the prevailing physical process during deposition in middle-shoreface settings, such that the majority of sedimentary structures, including hummocky cross-stratification, reflect storm deposition (e.g., Suter 2006).

An important paleoecological point to note is the potential difference in time averaging experienced by fossil assemblages in this facies. Fossil assemblages preserved on a single bed base in this facies can be assumed to represent contemporaneous organisms from the time of burial, as they are all smothered by sediment deposited by the same temporal event. However, since individual sand beds are discontinuous (Fig. 14B), of limited lateral extent, and deposited by episodic events, substrates could feasibly be only partially covered by any one event bed, such that any individual bed top surface may encompass fossils that were buried at different points in time by different event beds. This distinction has implications for paleoecological studies, since in order to apply techniques such as spatial point process analyses (SPPA; e.g., Mitchell and Butterfield 2018), studied surfaces need to reflect single populations of demonstrably contemporaneous organisms. Such studies should therefore be restricted to bed-base assemblages in this facies, to ensure that the assumption of a single community remains valid.

Facies 7: Multidirected Trough- and Planar-Stratified Sandstone

Sedimentology.—This medium- to coarse-grained, compositionally mature sandstone facies comprises 10 to 185 cm-thick beds that are tabular over the lateral extent of all studied outcrops (Fig. 16A). Beds have erosional basal contacts and display planar stratification (Fig. 16B), low-angle cross-stratification (Fig. 16C), and planar and trough cross-stratification (Fig. 16D, E). Planar stratification regularly passes upwards into cross-strata (Fig. 16F). Only individual sets of cross-stratification occur, with set thicknesses ranging from 8 to 60 cm. On rare occasions, sandstone tops are reworked by wave ripples (Fig. 16G). No mudstone partings are present, either on foresets or in between individual beds. At Moralana, this facies additionally contains compositionally immature granules in a medium-grained sandstone matrix (Fig. 16H). Spherical, possibly siliceous concretions occur throughout this facies association, often in high densities (Fig. 17A). Paleocurrent data from cross-strata have high dispersion, but a modal SW/SSW direction (Fig. 17E).

Paleobiology.—No ichnological or microbial signatures were observed. Holdfast taxa such as *Aspidella* have been noted previously by Reid et al. (2020). Gehling and Droser (2013) additionally note *Rugoconites*,
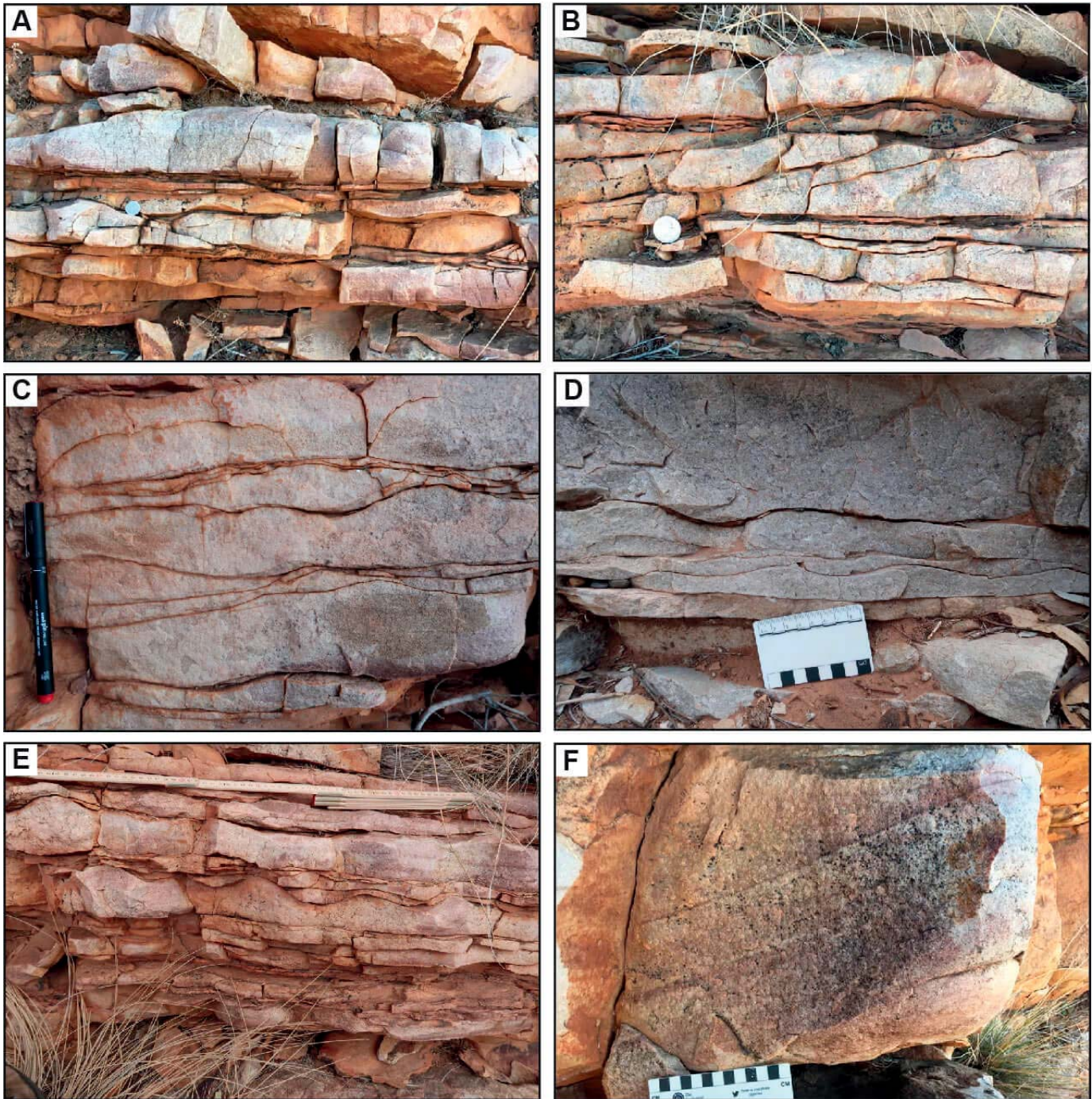
FIG. 14.—Sedimentary structures in Facies 6. **A–E)** Examples of erosionally amalgamated, discontinuous beds of sandstone with millimeter-thick siltstone or fine sandstone interbeds. A, B) Brachina Gorge. C) Bunyeroo Gorge. D) Moralana. E) Wilpena Pound. **F)** Unidirectional cross-stratification. Brachina Gorge. Coin diameter is 28.5 mm. Pen is 14 cm long. Rule for scale in Part E is 1 meter long.

Tribrachidium, *Dickinsonia*, and *Arborea*, although it cannot be stated with certainty whether these genera (from their "shoreface" facies) originate from the facies we describe here. In this study the only fossil specimens identified were poorly preserved *ex situ Aspidella* (Fig. 17B). Such specimens are evidently current-perturbed, with attached stalks showing current alignment (better examples of current-perturbed *Aspidella* are figured in Tarhan et al. 2015, their Fig. 5B).

Interpretation.—Well-preserved cross-bedding suggests shallow, active waters considerably above effective fair-weather water base. Multi-directed trough cross-stratification (Fig. 17E) is consistent with deposition on the upper shoreface (Davis 1978; Reinson 1984), which comprises the high-energy build-up and surf zone located between the breaker zone and the low-tide mark (Pemberton et al. 2012; Reineck and Singh 2012) (Fig. 2). The presence of low-angle cross-stratification
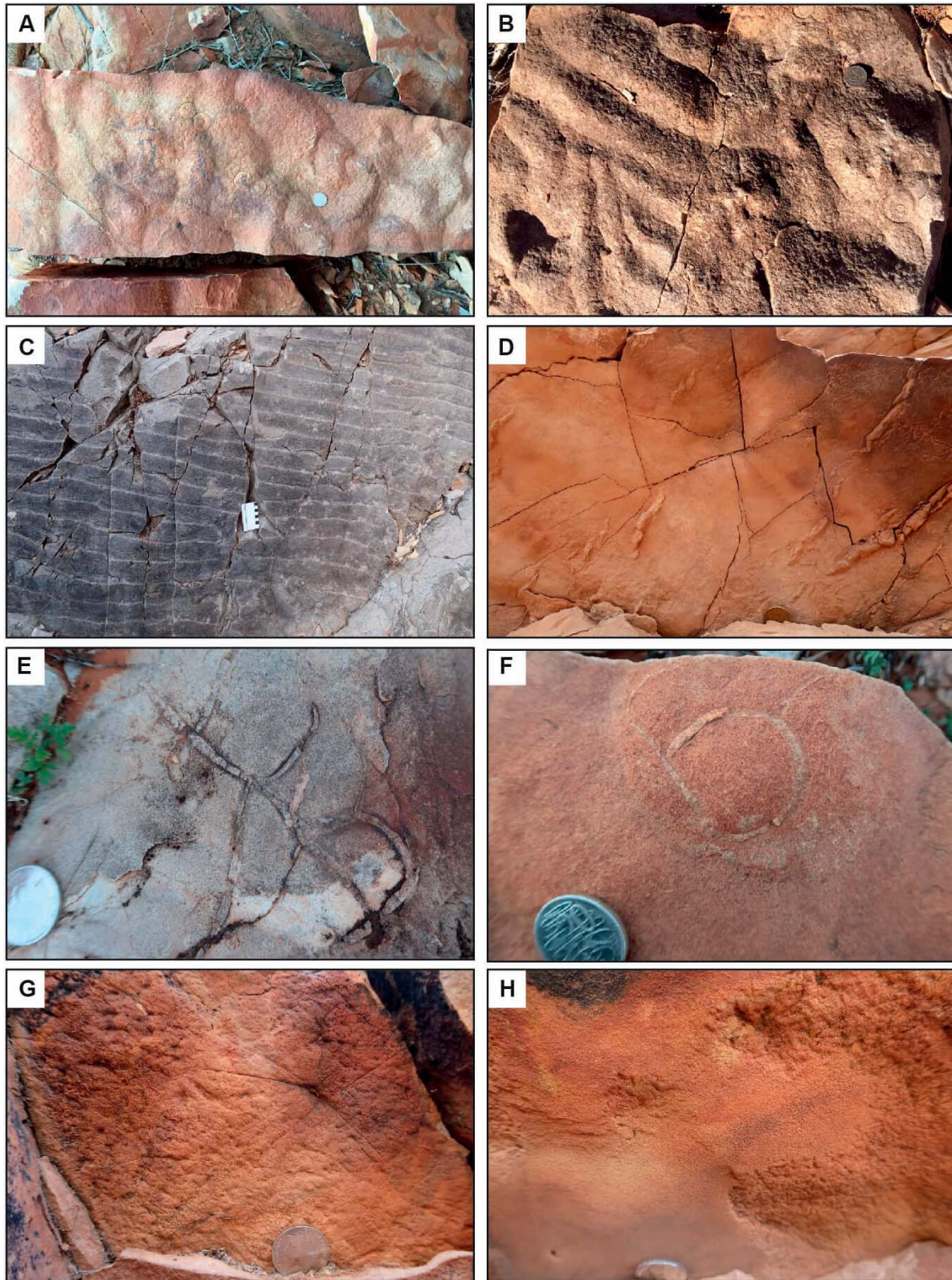
FIG. 15.—Sedimentary structures in Facies 6. **A)** Discoidal fossils assigned to "*Aspidella*" preserved on a true substrate with discontinuous ripple marks. Brachina Gorge. **B)** Interference patterns on rippled surfaces containing *Aspidella*, emphasizing a shallow-water origin. Brachina Gorge. **C)** Straight, unidirectional current-ripple marks. Brachina Gorge. **D–F)** Subaqueous shrinkage cracks at Bunyeroo Gorge (Part D), Brachina Gorge (Part E), and Moralana (Part F). **G)** *Coronacollina* preserved on a true substrate that displays "elephant-skin texture" microbial fabrics. Brachina Gorge. **H)** "Pucker" texture. Brachina Gorge. Coin diameter is 28.5 mm.
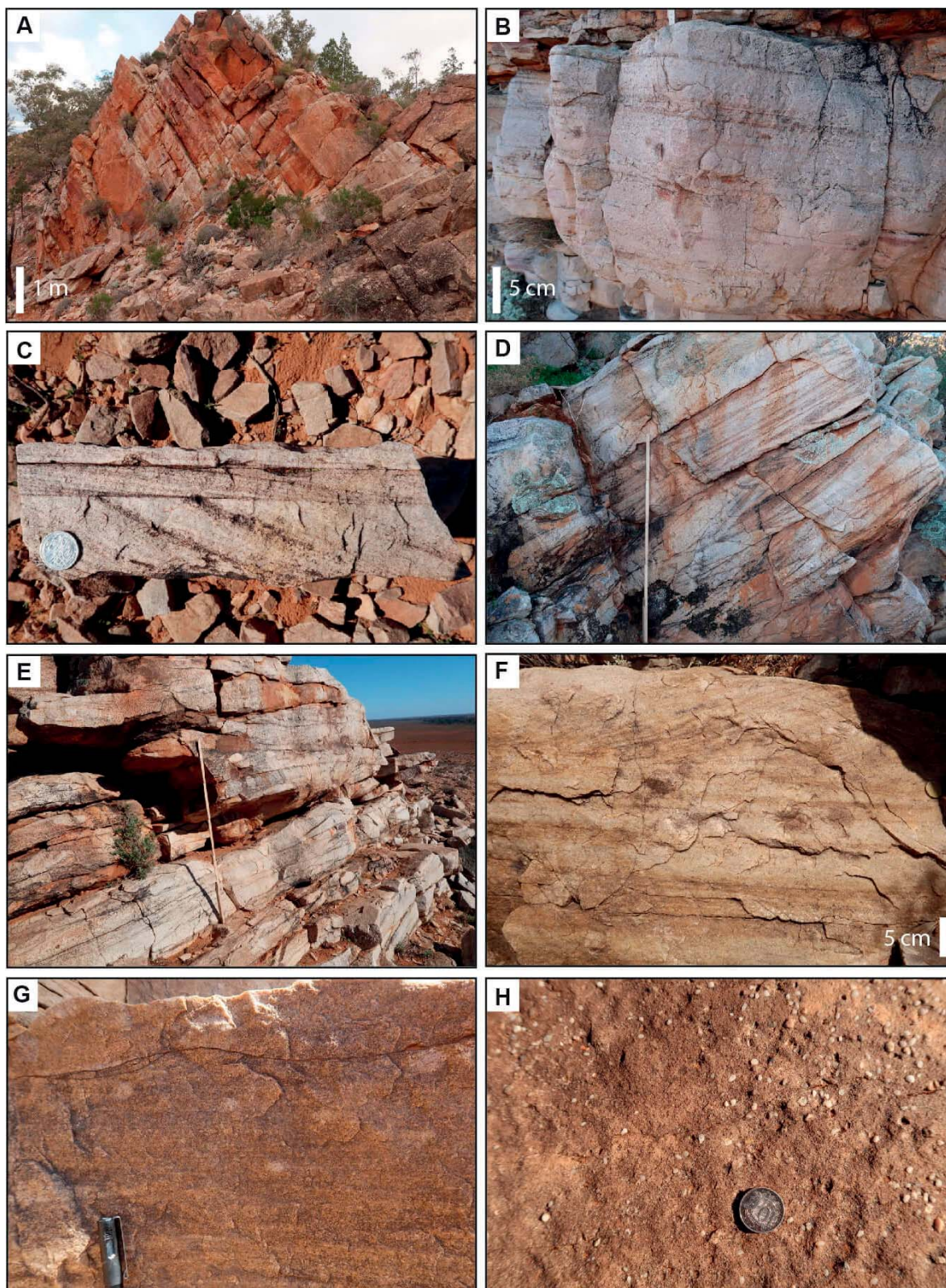
F𝑖ɢ. 16.—Sedimentary structures in Facies 7. **A)** Thick succession of Facies 7. Bunyeroo Gorge. **B)** Planar stratification. Brachina Gorge. **C)** Tangential cross-stratification erosionally overlain by low-angle cross-stratification. Brachina Gorge. **D–E)** Trough-cross-stratification. Moralana. **F)** Planar stratification transitioning upwards into trough-cross-stratification. Wilpena Pound. **G)** Planar stratification reworked by wave ripples. Brachina Gorge. **H)** Scattered granules in medium-grained sandstone matrix. Moralana. Coin diameter is 28.5 mm. Pen lid is 2 cm long. Rule for scale in Parts D and E is 1 meter long.
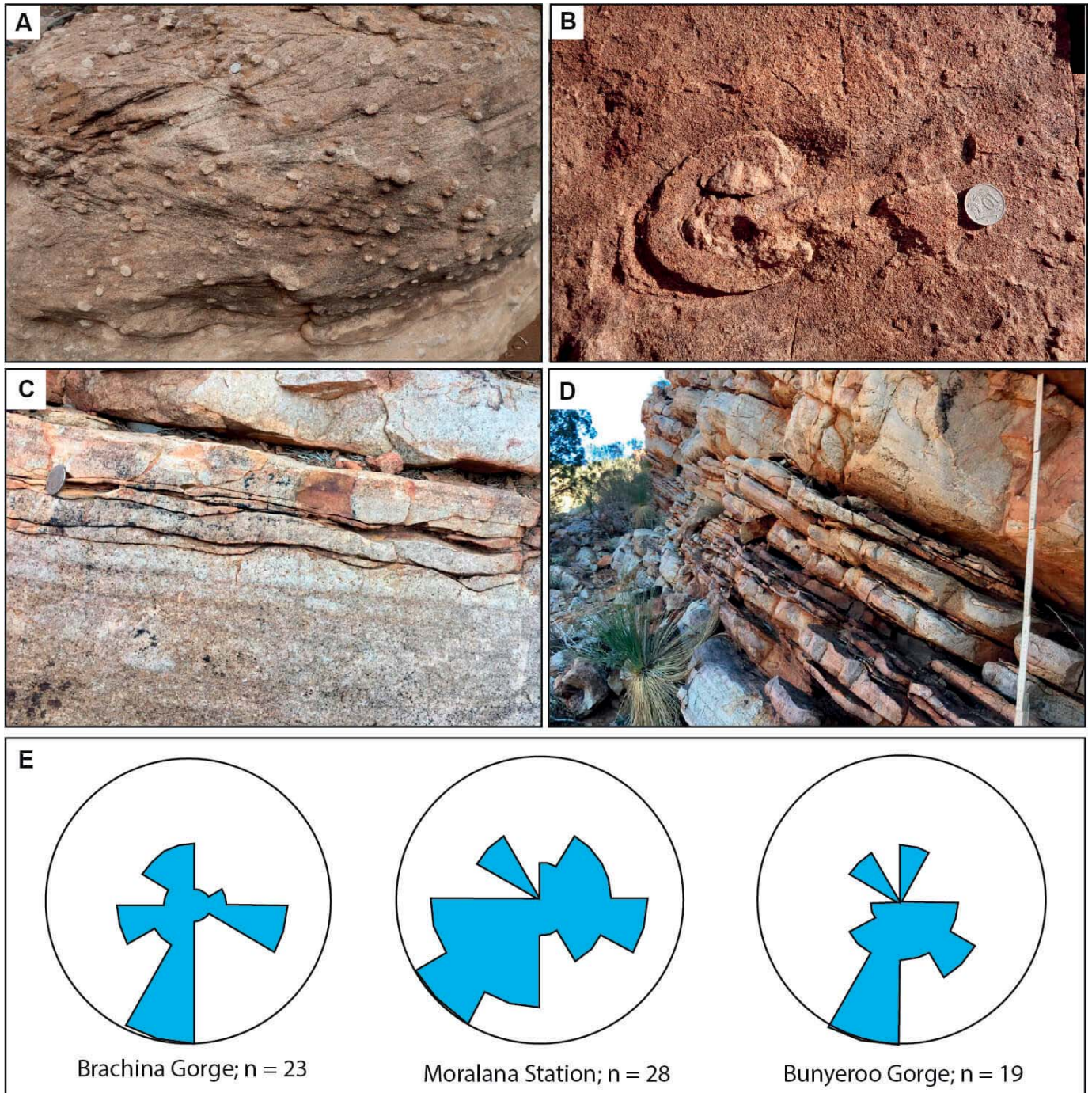
FIG. 17.—Sedimentary structures and paleoflow data from Facies 7. **A)** Spheroidal concretions widely associated with (but not unique to) Facies 7. **B)** Deformed *ex-situ Aspidella*-like holdfast discoidal fossil. **C**, **D)** Intercalation between Facies 6 and 7, suggesting that these two environments were temporally variable and proximally situated. Brachina Gorge. **E)** Representative paleoflow data measured from Facies 7. Coin diameter is 28.5 mm. Rule for scale in Part D is 1 meter long.

abruptly overlying cross-stratified sets (Fig. 16C) evidences the influence of wave swash (Pemberton et al. 2012). Modal SW and SSW-directed cross-beds may indicate the landward direction (Dashtgard et al. 2012), and are not dissimilar from the variably spread trough-cross-bedding azimuths measured previously from this facies south of Parachilna Gorge (Gehling 2000, his Fig. 4). Planar cross-stratification demonstrates the development of 2D dunes, whereas planar stratification indicates upper-flow-regime conditions. Regular upward transitions from supercritical to subcritical bedforms (Fig. 16F) demonstrate waning flow conditions, most likely due to a reduction in strength of tidal currents. Rippled tops likely developed during falling tide and low tide. Intercalation with the oscillation-ripple facies (Facies 6) indicates a gradational temporal transition between these two shoreface environments (Fig. 17C, D). Storm events in the upper shoreface are typically erosional, with reworked sediment transported and redeposited in more distal shoreface environments (such as Facies 5 and 6).

Whilst exercising reasonable caveats of uncertainty, estimates of maximum depositional water depth in the upper shoreface can be calculated using preserved trough-cross-set thickness. Preserved trough foresets for sandy dunes are most regularly on the order of a third of the formative dune height (e.g., Leclair and Bridge 2001; Julien et al 2002). Observed cross-set thicknesses in Facies 7 of 8 to 60 cm (average = 16 cm) therefore suggest dune heights between 24 and 210 cm. Using the relationship *water depth = 6.7 × dune height* established by Bradley and Venditti (2017), maximum water depths for this facies are estimated to be between 1.6 and 12.1 meters (average 3.2 meters).

Facies 8. Ripple Cross-Laminated, Horizontally Stratified Sandstone with Ripple Marks

Sedimentology.—Facies 8 is composed almost entirely of medium- to fine-grained sandstone, which in hand specimen appears to be more feldspathic than the underlying quartz-rich facies (Facies 5 to 7). Small-scale ripple cross-lamination dominates internal bedding (Fig. 18A, B), with laminae sometimes showing minor soft-sediment deformation (Fig. 18C). Planar stratification and low-angle cross-stratification also occur frequently (Fig. 18D, E). Planar and trough cross-bedding is uncommon (Fig. 18F), and intraformational sand clasts identical to those present in Facies 1 and 5 occur occasionally (Figs. 13F, 18G). Small (20 to 40 cm) barform deposits occur on very rare occasions, with discrete bottomset and asymptotic foreset elements, implying near-complete preservation (Fig. 18H).

Abundant symmetrical and asymmetrical ripple marks occur (Figs. 19, 20), with bedding planes hosting a broad diversity of ripple types including ladder (ripples with double crests) (Fig. 19D), rhomboid (Fig. 19E), straight-crested (Fig. 19F, G), sinuous (Fig. 19F), undulatory (Fig. 19H), and linguoid (Fig. 20A). Modified ripples (Fig. 20A), drainage lines (Fig. 20B), and interference marks (Fig. 20C) are widespread across the studied successions. Flattened ripples are present on rare occasions (Fig. 20D). Adhesion marks are also widely associated with ripple marks on certain bedding planes, either blending into trains of ripples (Fig. 20E) or occurring directly above ripple crests (Fig. 20F, G). Desiccated polygons were recognized in a single incidence of observed mudstone in the facies (Fig. 20H). Irregular to polygonal cracks in sandstone deposits also occur infrequently (previously referred to as "petee structures" (Gehling 2000) (Fig. 21A)).

Paleobiology.—There are no convincing examples of Ediacaran macrofossils in this facies, but rare concentric circular structures (Fig. 21B, C) and thin, positive-epirelief filamentous strands up to 1 mm in width (Fig. 21D) were observed. The circular structures do not closely resemble known holdfasts of *Aspidella*-type discs, but they appear to be primary structures, and are poorly preserved, so such original affinities cannot be categorically refuted. The filamentous impressions closely resemble late Ediacaran filamentous impressions from Newfoundland, Canada (Callow and Brasier 2009; Liu et al. 2012), some of which can be intimately associated with frondose taxa (Liu and Dunn 2020), but such impressions here could alternatively reflect algal or bacterial remains. On rare occasions, irregular "lozenge" shaped features confined to ripple troughs occur on sandstone bedding planes (Fig. 21E). Similar features have been reported by Prave (2002) and McMahon and Davies (2018b) and interpreted as possible fragments of microbially bound sand layers that had undergone entrainment and rolling during flow. Alternatively, these textures may represent remnant fragments of *Manchuriophycus* cracks, described previously from this facies (Gehling 2000, his Fig. 7G), also confined to ripple troughs (e.g., McMahon et al. 2017b), and frequently thought to form as a result of the shrinkage of microbial mats with very high strengths and elasticity (Koehn et al. 2014). Cracks in pure sandstone may also have required microbial assistance to form (McMahon et al.

2017a). Elephant-skin texture, similar to that described in Facies 6, is also rarely seen on Facies 8 rippled surfaces (Fig. 21F). Intraformational sand clasts have the same potential rip-up microbial mat origin as described in Facies 5.

A small number of simple horizontal surface trace fossils, similar to those referred to as *Helminthoidichnites* by other authors, were observed on a current-rippled sandstone at the north end of Moralana Scenic Drive (Fig. 21G), occurring at the same stratigraphic horizon as an adhered and cracked bedding plane (Fig. 21H). These trace makers were demonstrably active on foreshore surfaces subject to intermittent emergence (though were not necessarily themselves active during subaerial exposure (see Shillito and Davies 2018)). The colonization of land was a major event in the history of life, and if confirmed, this discovery extends the known record of motile invertebrates in coastal environments from the Cambrian (e.g., MacNaughton et al. 2002; Hagadorn et al. 2011; Collette et al. 2010) back into the Ediacaran.

Interpretation.—Facies 8 is best interpreted as representing deposition along the foreshore (i.e., regions located between the high- and low-water level line) (Fig. 2). Sandstone dominance may be due to the foreshore's location immediately landward of the open shoreface complex. Such areas would be subjected to significant fair-weather wave activity, perhaps sufficient to prevent long-term mud retention (Van de Lageweg et al. 2018). The increased feldspar content is consistent with a decreased attrition rate of labile minerals compared with the laterally equivalent, overall higher-energy nearshore marine environments represented by Facies 5 to 7 (e.g., Martens 1931; Went 2013). Abundant adhesion marks blanketing many deposits demonstrate that the foreshore was also prone to mud-stripping wind erosion. Reworking by these processes may have been favored by the absence of baffling vegetation (e.g., Tirsgaard and Øxnevad 1998). Other evidence of emergence includes petee lamination: syndepositional domed and disrupted laminae that developed in the absence of mud (Fig. 21A) (Gehling 2000).

Planar stratification may represent swash-zone processes on the foreshore (Pemberton et al. 2012), with rare planar cross-bedding indicating the migration of 2D dunes, possibly during storm events. Occasional soft-sediment deformation in ripple cross-laminated sandstones potentially reflects storm activity (Fig. 18C). Symmetrical ripple marks are interpreted as the result of wave currents acting above a sand sheet in shallow water. Rhomboid ripples (Fig. 19E) are typical of modern foreshore environments (e.g., Chakrabarti 2005). Ladder ripples (Fig. 19D) may be characteristic features of falling water level, with the larger ripples forming during high-water stage and superimposed smaller crests during low stage. Evidence for intermittent emergence includes drainage lines etched into ripple flanks, demonstrating drainage processes subsequent to ripple formation (Fig. 20B). The high disparity in ripple-direction strike line, in addition to successive sets often showing entirely different trends (Fig. 19A, B) demonstrate drainage of ponded water in multiple directions, most probably due to localized slopes, alternating tides, and shifting wind directions. Adjacent ripples with identical strike lines but a pronounced difference in crest height (Fig. 19G) indicate rapid wave-height decline such that period doubling in ripple forms occurred (Doucette and O'Donoghue 2006). Widespread interference patterns demonstrate common modification of the same sedimentary substrate.

Facies 8 bedding planes, which archive intricately preserved sedimentary surface textures that formed at the time of deposition, can be defined as "true substrates" (Davies and Shillito 2018). Recent work attests that the preservation of such high-resolution original morphology requires no unusual circumstances, with the occasional preservation of true substrates an inevitability of the interplay between the ordinariness, sedimentary stasis, and spatial variation that sculpt the siliciclastic record (e.g., Miall 2015; Tipper 2015; Davies et al. 2017, 2019; Shillito and Davies 2020). Notions that delicate sedimentary surface textures (e.g., adhesion marks,
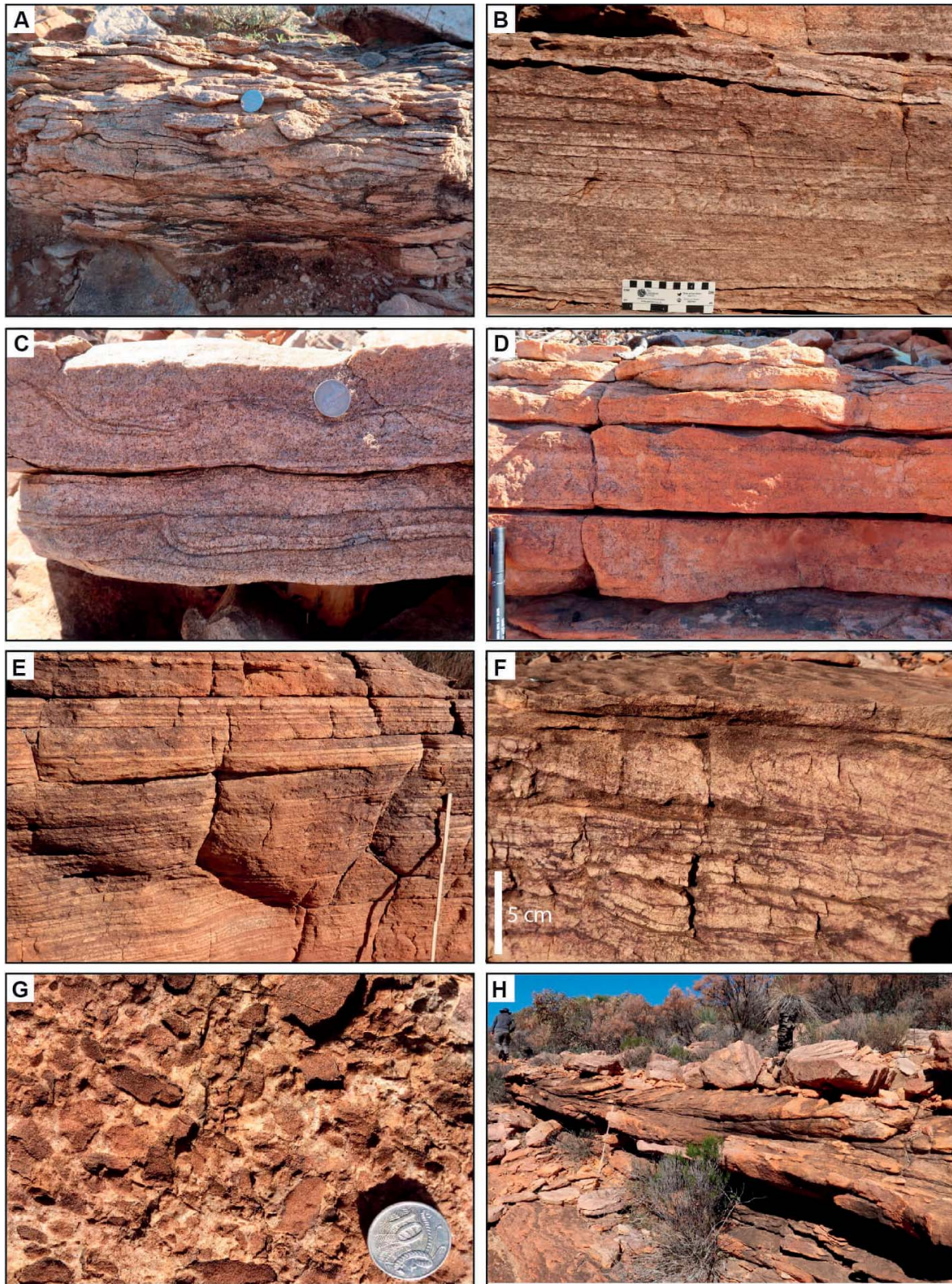
FIG. 18.—Sedimentary structures in Facies 8. **A, B)** Ripple cross-lamination at (Part A) Moralana and (Part B) Brachina Gorge. **C)** Lamina-scale soft-sediment deformation. Moralana. **D)** Horizontal-stratification with wave-reworked surface. Wilpena Pound. **E)** Horizontal-stratification. Brachina Gorge. **F)** Planar-cross-stratification. Moralana. **G)** Intraformational sand-clasts. Moralana. **H)** Top-truncated barform deposits. Foresets become slightly tangential towards top-truncation, implying the barform deposits are close to fully preserved. Wilpena Pound. Coin diameter is 28.5 mm. Pen is 14 cm long. Rule showing in Part E is 50 cm long, and in Part H is 1 meter long.
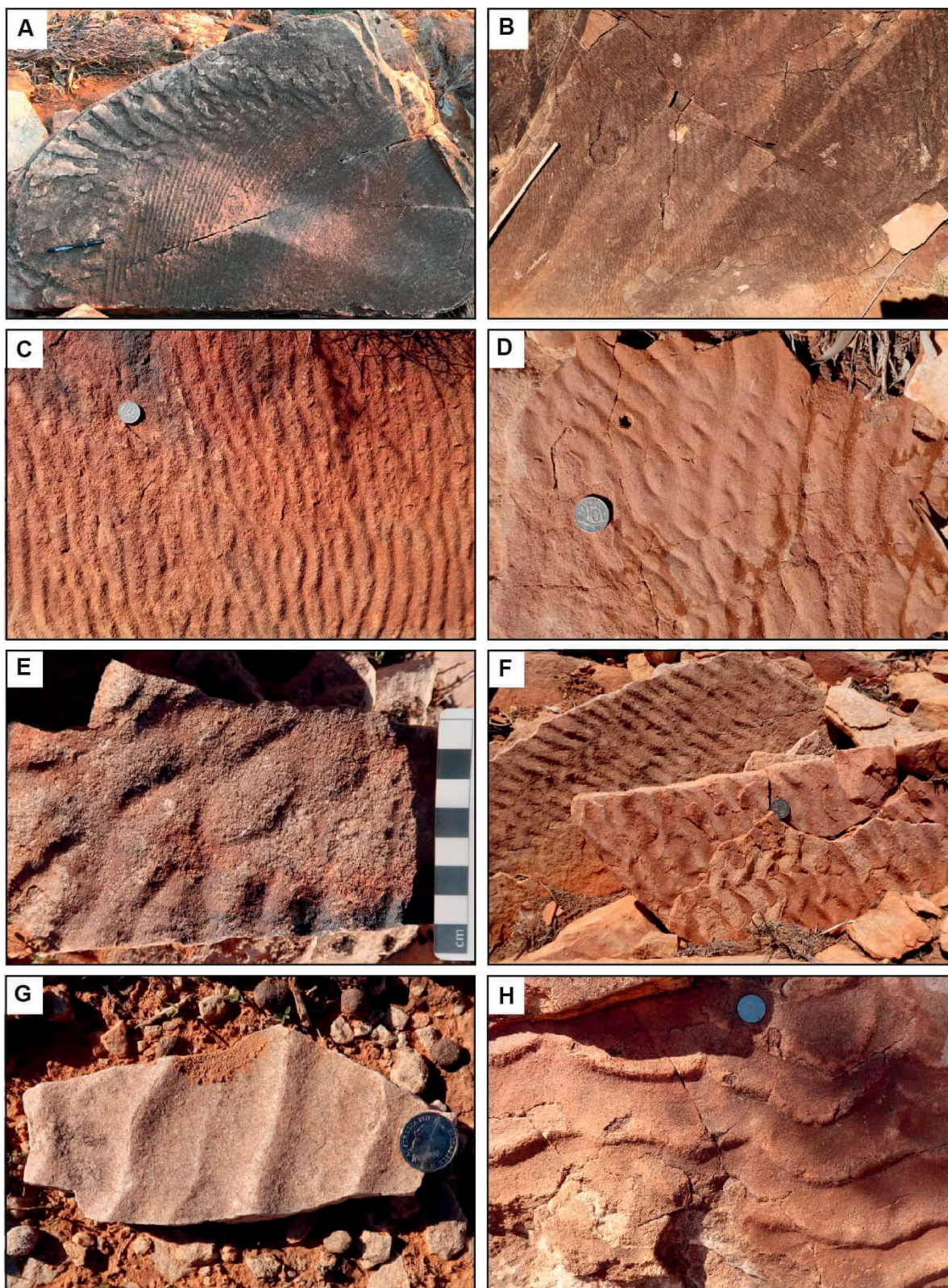
Fig. 19.—Ripple marks preserved on true substrates in Facies 8. **A**, **B)** Vertically juxtaposed curved ripple crests displaying different strike lines at (Part A) Brachina Gorge and (Part B) Wilpena Pound. **C)** Straight-crested ripples. Brachina Gorge. **D)** Ladder ripples. Brachina Gorge. **E)** Rhomboid ripples. Moralana. **F)** Sinuous ripple marks. Wilpena Pound. **G)** Straight-crested ripples with markedly different crest heights. Moralana. **H)** Undulatory ripples. Bunyeroo Gorge. Coin diameter is 28.5 mm. Ruler is 20 cm long.
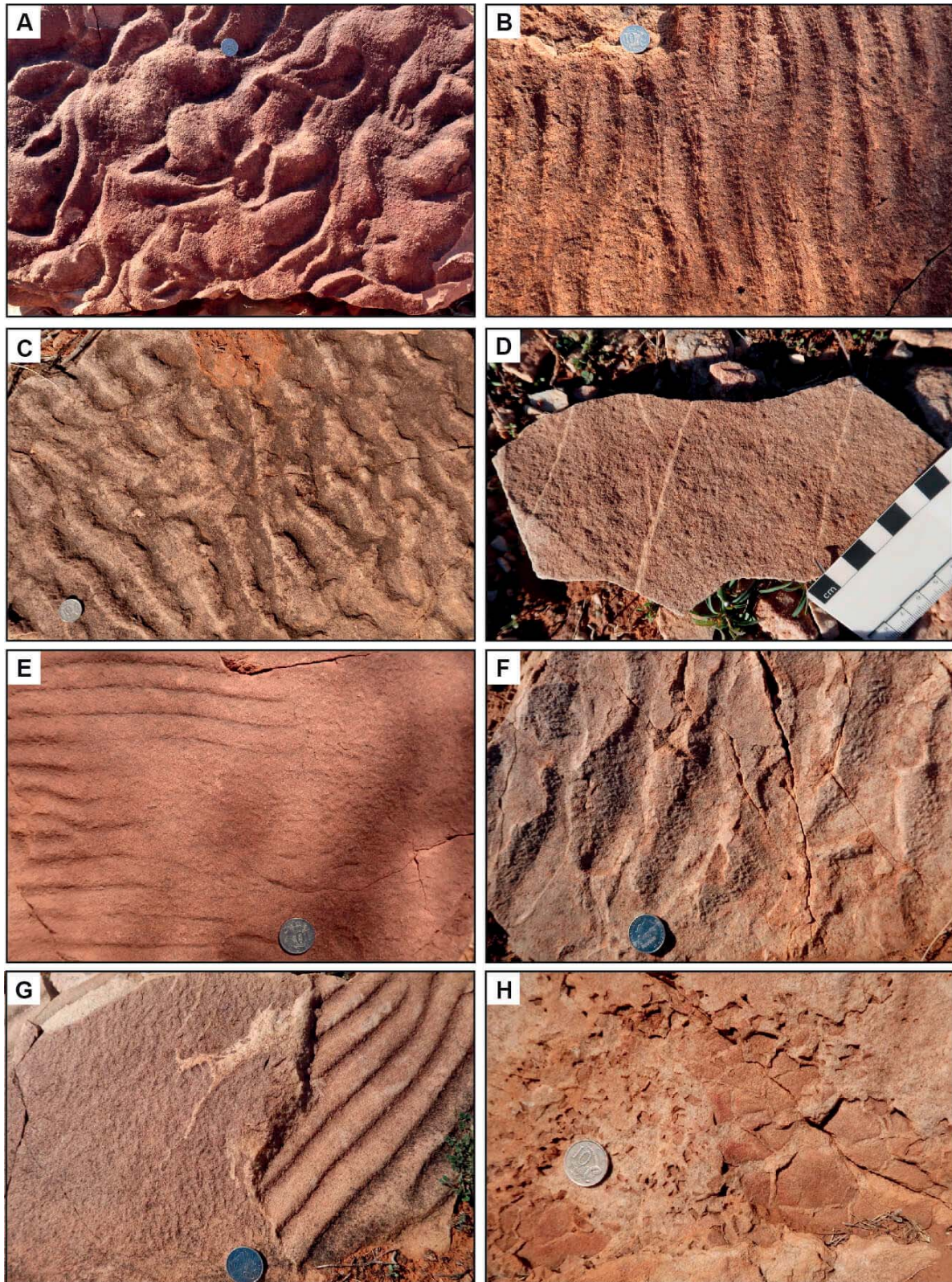
FIG. 20.—Sedimentary structures in Facies 8. **A)** Linguoid ripples. Brachina Gorge. **B)** Ripple marks with etched drainage lines. Brachina Gorge. **C)** Interference ripple marks. Brachina Gorge. **D)** Flattened unidirectional ripples. Moralana. **E)** Ripple marks merging into adhered sandstone. Brachina Gorge. **F)** Adhered asymmetrical ripple marks. Moralana. **G)** Blanket of adhesion marks covering rippled surface. Moralana. **H)** Desiccation cracks. Brachina Gorge. Coin diameter is 28.5 mm.
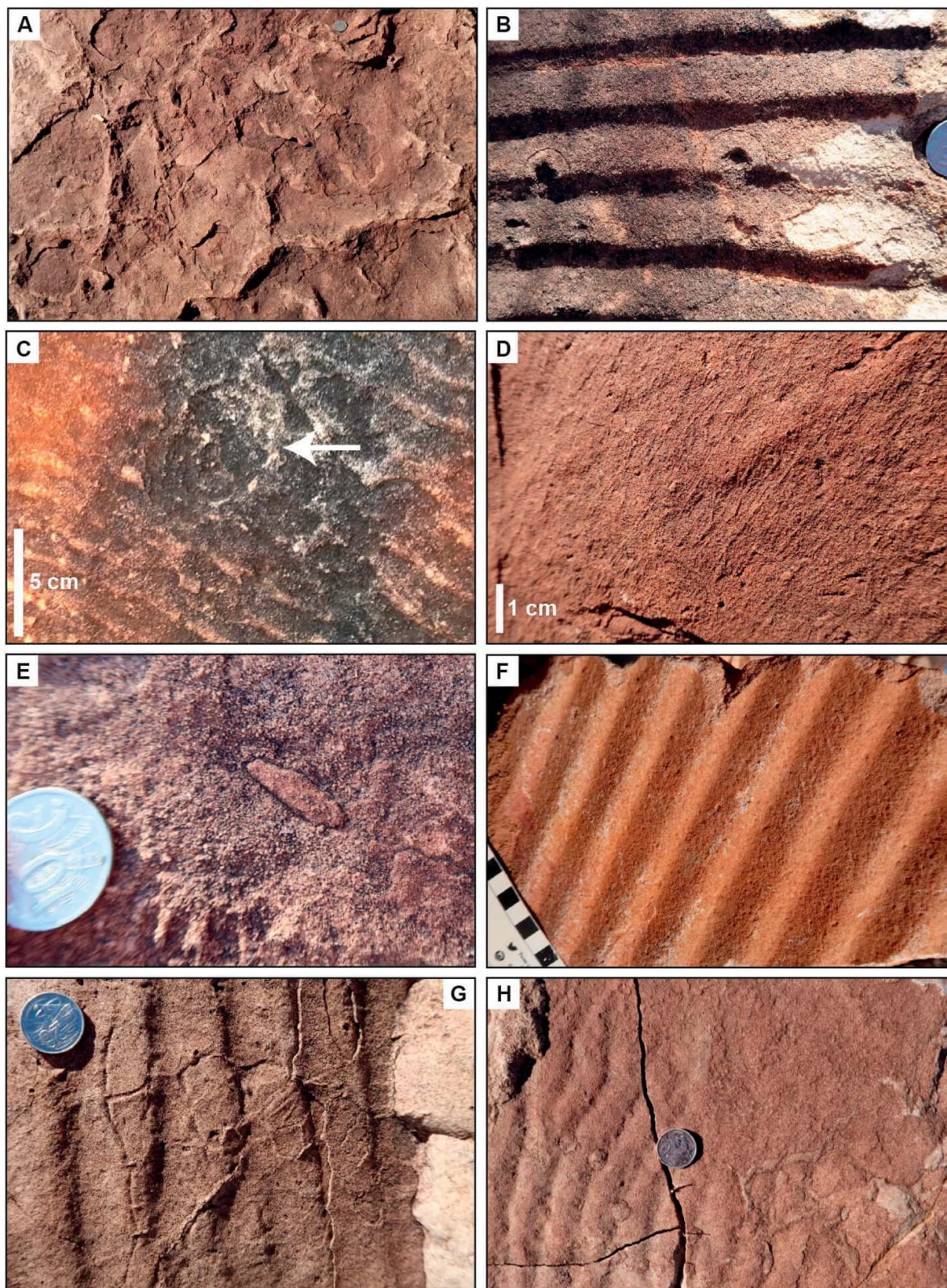
FIG. 21.—Sedimentary structures and possible fossils in Facies 8. **A)** Sandstone cracks (described as petee structures by Gehling 2000). Brachina Gorge. **B**, **C)** Concentric circular structures in current-ripple sandstone. Brachina Gorge. **D)** Positive-epirelief filamentous-like strands. Brachina Gorge. **E)** "Lozenge" shaped feature in ripple trough. Brachina Gorge. **F)** Ripple marks covered in "elephant-skin" texture. Brachina Gorge. **G)** Simple horizontal surface trace fossils on emergent bedding plane. Moralana Scenic Drive. **H)** Adhered and cracked sandstone bed at the same stratigraphic horizon as horizontal trace fossils in Part G. Moralana Scenic Drive. Coin diameter is 28.5 mm.

ripple marks) require the aid of microbial cohesion of sediment for preservation (in the Rawnsley Quartzite and elsewhere) (e.g., Gehling 2000; Seilacher 2008; Sarkar et al. 2011; Sappenfield et al. 2017; Tarhan et al. 2017; Bradley et al. 2018; MacNaughton et al. 2019) are unnecessary. This point may also apply to the presence of macrofossils on such substrates (see Bobrovskiy et al. 2019, and later discussion).

Facies 9. Adhered Sandstone

Sedimentology.—This sandstone facies consists of fine- to medium-sand-size, very well sorted grains. Adhesion ripples (Fig. 22A–C), adhesion marks (Fig. 22D, E) and planar-laminated sand (Fig. 22F) are the dominant bedding structures. Individual adhesion marks present as 2 to 5 millimeter-wide, 1- to 3-millimeter-high positive-epirelief mounds. Planar laminae form thin (< 5 mm) ungraded sets usually less than 5 cm thick.

Paleobiology.—No paleontological, ichnological, or microbial signatures were recognized in Facies 9.

Interpretation.—The dominance of aeolian bedforms and close association with facies consistent with deposition along the upper-shoreface to foreshore complex (Facies 7, 8) suggest that Facies 9 represents deposition in a beach backshore environment. It is distinct from Facies 8, which also contains adhered sandstone, in lacking evidence for intermittent subaqueous deposition. Unlike the foreshore, which undergoes regular submergence, backshore environments represent the upper part of a beach and normally remain dry except under unusually high waters (Reineck and Singh 2012). Over geological timescales these environments would have regularly shifted within any one location, as demonstrated by the close intercalation of Facies 8 and 9 (Figs. 3, 4). Rare coastal dunes are potentially preserved as erosionally based cross-stratification, although fields of coastal sand dunes, perhaps expected somewhere in the Rawnsley Quartzite outcrop belt, are yet to be identified.

Facies 10. Planar-Stratified and Cross-Stratified Sandstone with Ripple Cross-Lamination

Sedimentology.—This facies is observed predominantly in the uppermost sections at Brachina Gorge, where over 50 m of stratigraphy consists of quartz-rich, medium- to coarse-grained cross-stratified sandstones (Fig. 22G). This thick facies remains understudied and is a topic of ongoing research, with only an initial examination of the sedimentology presented here. Facies 10 is distinct from Facies 7 (trough-cross-stratified and horizontally stratified sandstone) in that cross-bedding comprises both planar- and trough-cross forms, as well as the additional presence of ripple cross-lamination near some bed tops. Many beds have a topset comprising a 1- to 10-centimeter-thick set of planar stratification, which often coarsens upwards from medium to coarse sand (Fig. 22H). Observed channelized scours occasionally occur and have a cross-stratified fill (Fig. 11C). True substrates are absent, with bedding contacts always erosional.

Paleobiology.—No paleontological, ichnological, or microbial signatures were observed in Facies 10.

Interpretation.—Facies 10 is suggested to have formed in broad, shallow distributary channels entering the shoreface. Subcritical bedforms record nearshore tidal dunes, which became washed out when water depth shallowed (Fielding 2006). The absence of true substrates limits the biological information attainable from the facies (see Paleobiological Implications), although the actively depositing environments may well have been unsuitable habitats for Ediacaran taxa.

STRATIGRAPHIC ORGANIZATION

In our view, the Ediacara Member and the Upper Rawnsley Quartzite facies can be organized into four coastal to shallow-marine depositional complexes (Fig. 23): 1) a tide-dominated estuary, 2) a prograding marine shoreface complex, 3) a stacked foreshore to backshore complex, and 4) prograding distributary channels. Each complex reflects discrete combinations of physical processes, some of which enabled proliferation, or more precisely, preservation, of Ediacara biota communities.

Complex 1: Tide-Dominated Estuary

This facies succession begins at the contact of valley-wide stratigraphic discontinuities, with erosion into the underlying Chace Quartzite occurring during the previous lowstand (Gehling 2000). The initial (Facies 1) deposits that constitute the subsequent transgressive systems tract accumulated as incised valleys were converted into estuaries following marine flooding. Estuaries differ from deltas in receiving sediment from both fluvial and marine sources, with their identification in ancient stratigraphy usually dependent on the recognition of associated incised valleys (Dalrymple et al. 1992). Conversely, Gehling (2000) used the recognition of incised valleys and type 1 sequence boundaries (Vail et al. 1984) as evidence to dispute the previous estuarine model of Jenkins et al. (1983), and proposed deeper-water submarine channel environments. In coastal settings characterized by rapid transgression, lowstand fluvial and estuarine deposits may not be preserved, with the initial fill instead consisting of highstand fluvial or shallow-marine deposits (Catuneanu 2006). Initial deposition of even deeper submarine flows would require a basinward shift of the previously emergent incised valleys to the seaward side of the submarine slope or staging area. Facies 1 sedimentary structures and stratigraphic context are more consistent with deposition as estuarine and tidally influenced river channels (e.g., Martinius and Van den Berg 2011). Preserved bar deposits are consistent with a wide tidal system (unconfined by salt-marsh vegetation as is the case in the present-day (Brückner et al. 2020)) such that a braided bar pattern might be expected. Bar length is strongly correlated to estuary width, with bar width in turn proportional to bar length (Leuven et al. 2016). The bar width relative to estuary width gives an indication of the degree of braiding. The preserved paleovalley at Bunyeroo Gorge (Fig. 1B) has a width of 1.2 to 1.5 km, suggesting the original valley may have held bars up to 600 m long and 100 m wide. Assuming a lack of cohesive banks and bar tops, this environment would have been highly dynamic with regularly shifting channels. The estuarine channel deposits either pass upwards into intertidal mixed-flat environments (Facies 2) or the red sandy siltstones that may have accumulated in lagoons or interdistributary bays (Facies 4). Whereas the studied Ediacara Member estuarine deposits (Facies 1 and 3) are devoid of macrobiota (but also only scarcely contain true substrates on which macrobiota would have a chance of becoming preserved), mixed-flat and lagoonal facies are not. Whilst Ediacaran macrobiota have recently been suggested to be preserved in tidal-flat facies elsewhere (Bobkov et al. 2019; Sozonov et al. 2019), the likely brackish-water conditions of these settings would not necessarily be expected to favor long-term survival of such organisms, given their typical inferred marine habitats, and such reports demand further investigation.

Complex 2: Marine Shoreface

Though significant intercalation occurs, shoreface deposits generally have an overall regressive stacking pattern (Fig. 3, 4), with deposits typically passing upwards from lower and middle shoreface to middle and upper shoreface settings. This stacking pattern indicates that whilst relative sea level may have been falling during deposition, accommodation space remained available. If Ediacara Member shoreface deposits are, like the underlying estuarine deposits, confined to previously developed incised
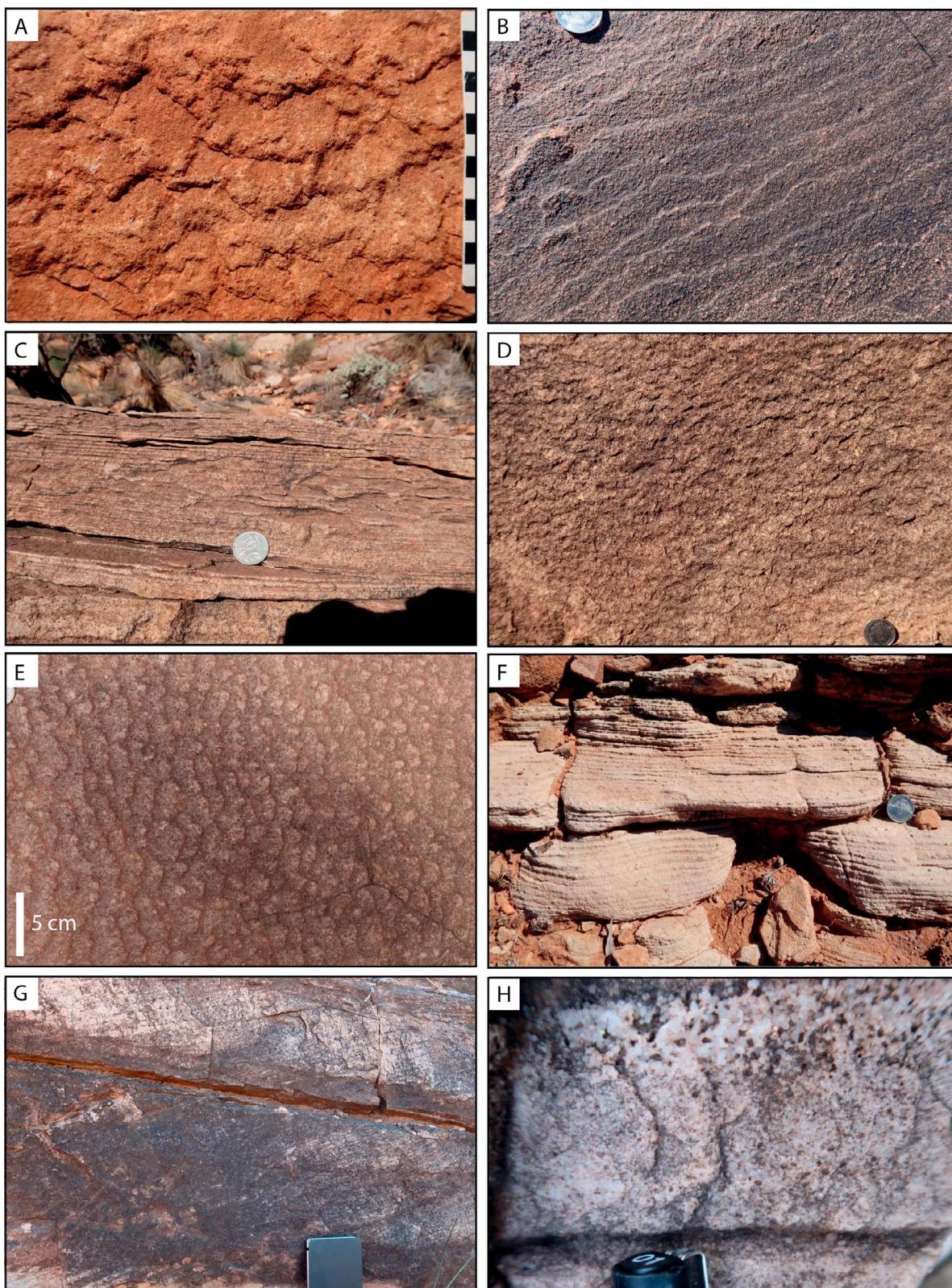
Fig. 22.—Sedimentary structures in Facies 9 (A–F) and 10 (G, H). **A, B)** Adhesion ripples at (Part A) Brachina Gorge and (Part B) Bunyeroo Gorge. **C)** Adhesion marks in vertical section. Brachina Gorge. **D, E)** Adhesion marks at (Part D) Moralana and (Part E) Bunyeroo Gorge. **F)** Planar stratified sandstone. Moralana. **G)** Planar cross-stratified sandstone. Brachina Gorge. **H)** Coarsening-upward pattern in planar stratified sandstone. Brachina Gorge. Coin diameter is 28.5 mm. Pen is 1 cm wide. Notebook is 20 cm long.
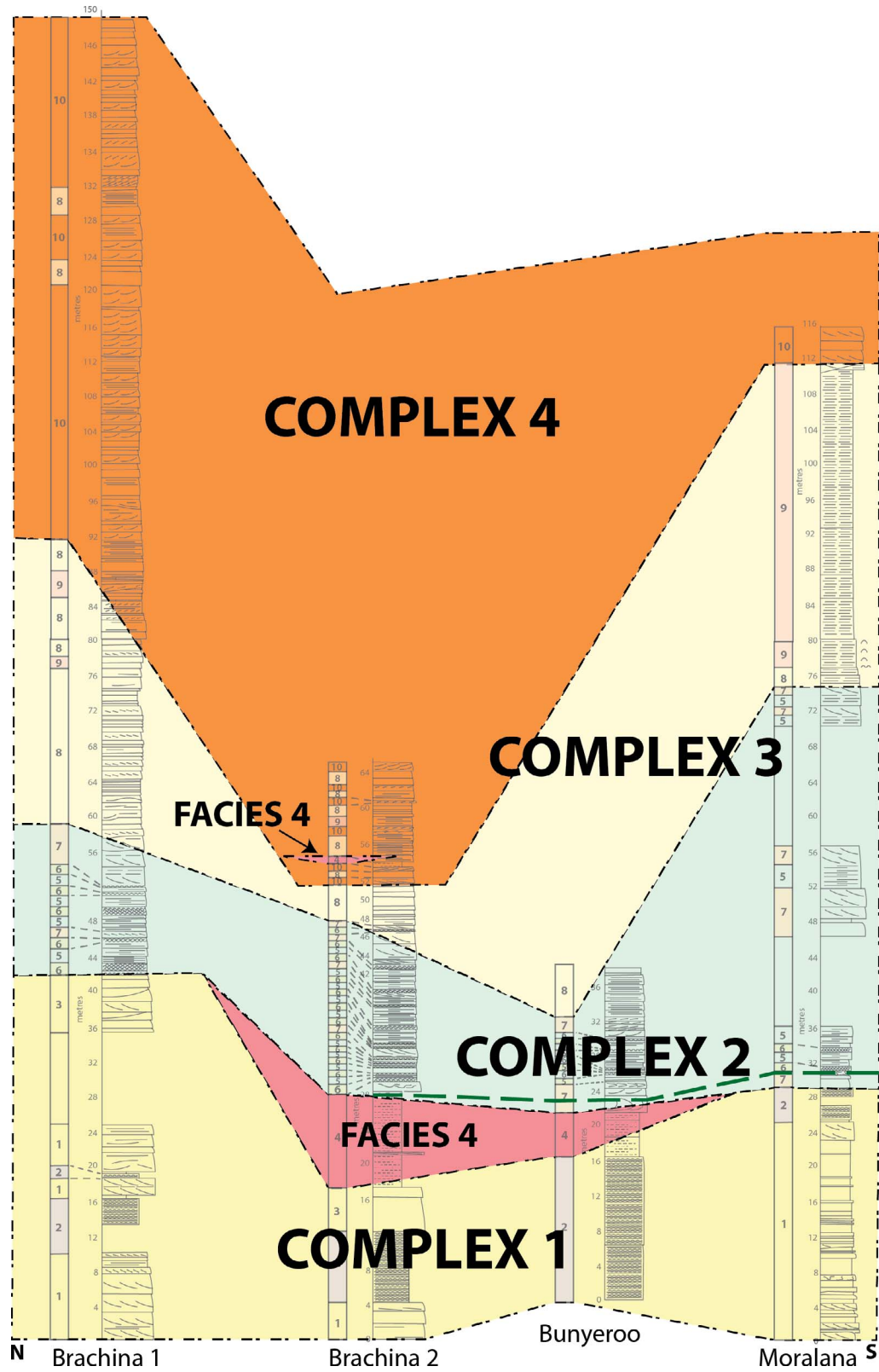
FIG. 23.—Cross section (approximate bases only) illustrating the detailed correlation of the Brachina Gorge, Bunyeroo Gorge, and Moralana sections. Note the lateral continuity of soft-sediment deformed-horizons (dashed green line), suggesting that deformation took place during one key event (potentially seismic). Key for symbols follows that used in Figure 3.

valleys, accommodation space was not entirely filled by the transgressive systems tract. Our interpretation of the Ediacara Member facies recognizes all body-fossil-bearing facies (Facies 2, 4, 5, 6, and 7) to be definitively marine (*contra* Retallack 2013). Previous models have suggested that the facies considered here represent deposition on a marine-shoreface complex accumulated entirely beneath effective fair-weather wave base (Gehling 2000; Gehling and Droser 2013; Tarhan et al. 2017; Reid et al. 2020). Treating geological successions as depositing above, between, or below fair-weather and storm-wave-base is useful for sedimentary facies models where particular water depths are associated with specific sedimentary characteristics. However, "wave bases" in modern environments are never as rigidly defined because of the variability in storm magnitude and frequency (e.g., environments subject to greater storm domination have deeper effective wave bases approaching maximum storm-wave base; Passchier and Kleinhans 2005; Pemberton et al. 2012). Consequently, deposits thought to be characteristic of "lower shoreface" settings may have in fact accumulated considerably below the effective fair-weather wave base. Regardless, previous researchers of the Rawnsley Quartzite have interpreted storm deposits (e.g., tempestites, oscillation ripples, hummocky cross-stratification) as reflecting settings entirely between the fair-weather and storm-wave base (e.g., Gehling 1999, p. 43). Oscillation ripples may occur in upper offshore environments between fair-weather and storm wave base, but are equally (or more) abundant along the marine-shoreface complex above fair-weather wave base (Boyd et al. 1988; Passchier and Kleinhans 2005). Hummocky cross-stratification, though still subject to controversy (Quinn 2011), is known from any marine environment impacted by storm deposition (i.e., above maximum storm-wave base). This includes not only offshore environments between storm and fair-weather wave base (e.g., Walker and Plint 1992; Passchier and Kleinhans 2005), but also shallower shoreface settings (e.g., Clifton 2003). In addition, sole marks and flat intraclasts of siltstone and sandstone may occur in any number of environments (Figs. 6G, H, 13E, 18G).

Complex 3: Foreshore to Backshore Complex

Complex 3 records deposition on open-coast foreshore and backshore environments. Limited mud-rich strata, such as flaser bedding or tidal bundles, may result from significant wave-reworking of the exposed flats (e.g., Amos 1995; Braat et al. 2017; van de Lageweg et al. 2018), possibly in conjunction with decreased availability of muddy sediments before the evolution of land plants (e.g., McMahon and Davies 2018a). No pronounced vertical facies trends are present in Complex 3 within the studied locations. Evidence for macroscopic biological activity is limited to rare trace fossils (Fig. 21G), with no clear body fossils identified.

Complex 4: Prograding Distributary Sands

Planar and trough cross-bedding become more abundant higher in the stratigraphy, and true substrates (Figs. 19–21) are replaced by erosional-bed junctions (e.g., Fig. 22G). This transition marks the onset of actively depositing distributary channels (Gehling 2000). Vertical association with foreshore environments (Complex 3), and the overall absence of channel forms, suggests that the studied deposits represent the seaward limit of distributary-channel networks. In such locations the formation of a sandy shoal occurs due to decreased current velocity as flow becomes unconfined (Reineck and Singh 2012). Decameter-thick successions of shoal deposits indicate that significant accommodation space was available during this stage of basin development (Fig. 3). The occurrence of red silty sandstones (Facies 4) vertically juxtaposed between cross-bedded distributary sand deposits (Facies 10) (Fig. 11C), emphasizes the shallow-water origin of the former, contrasting with the previously proposed sub-storm-wave-base depositional environment (Gehling and Droser 2013; Tarhan et al. 2017; Reid et al. 2020). The absence of body fossils and trace fossils in this

complex may result from the scarcity of true substrates on which they could become preserved.

Sequence-Stratigraphic Evolution

Studies of the Rawnsley Quartzite have considered all fossiliferous facies to be part of the Ediacara Member (Gehling 2000), defining the Ediacara Member as comprising all deposits from the base of the incised valleys carved into the underlying Chace Quartzite Member, to the top of the cross-stratified and planar stratified sandstone facies (i.e., Facies 1 to 7 in this study; Jenkins et al. 1983; Gehling 2000). The onset of Facies 8 foreshore deposition is considered a return to conditions typical of the unfossiliferous Chace Quartzite (Counts et al. 2016), with deposits consequently referred to as the upper Rawnsley Quartzite (Gehling 2000). A significant change in basin structure has been suggested to accompany this transition from the Ediacara Member to the Upper Rawnsley Quartzite, with the latter no longer being confined to incised valleys (Gehling 2000, his Fig. 2). There is no evidence for a stratigraphic hiatus between the Ediacara Member and the Upper Rawnsley Quartzite, with deposition of Facies 5 to 9 in this study archiving a gradational shift between laterally adjacent shoreface, foreshore, and backshore environments entirely consistent with Walther's law of facies (Walther 1894). Marked variations in succession thickness across our studied localities and the wider outcrop belt (Gehling 1982) are consistent with the filling of discrete paleotopographic lows as previously proposed (Gehling 2000). However, valley margins are only rarely traceable at outcrop (Fig. 1B), such that the depth of incision is based purely on the thickness of Ediacara Member facies at any individual location. It is possible that this methodology has led to overestimates of the depth of incision at certain locations, acting on the presumption that all Ediacara Member facies form part of a larger valley fill. Sequence boundaries, which might accompany the complete filling of an incised-valley (essentially an endorheic basin), may be difficult to identify without accurate geochronological or biostratigraphic constraint, or evidence of tectonic interference. It is not uncommon for Precambrian sedimentary formations to be poorly dated, with the Rawnsley Quartzite being no exception. Its inferred late Ediacaran age is based on its stratigraphic position beneath dated basal Cambrian sediments (Jago et al. 2012) and above the prominent Wonoka carbon-isotope anomaly (Grey and Calver 2007), and correlation of Ediacaran macrofossils with similar assemblages dated at ∼ 555 Ma from the White Sea of Russia (Martin et al. 2000). Without accurate dating, internal hiatuses in deposition might only be recognized by changes in tectonic dip, or vertical juxtaposition of spatially segregated environments. For example, Gehling (2000) recognized that the total duration of deposition of the Rawnsley Quartzite encompasses the accumulation of the lower Chace Quartzite Member, the time for erosion at the base of the Ediacara Member, and the subsequent deposition of the Ediacara Member and the Upper Rawnsley Quartzite (Facies 1 to 10). Whilst no evidence for any breaks in deposition are present between the shoreface to foreshore and backshore environments of Facies 5 to 9, other potential hiatal gaps do exist. For example, changes in tectonic dip are apparent between Facies 3 and 4 at Brachina Gorge (Fig. 10A), and in Facies 4 at Bunyeroo Gorge (Fig. 11D). These changes may represent breaks in deposition, possibly relating to filling of available paleovalley accommodation space.

Further study of basin structure and facies evolution is necessary and ongoing, particularly in relation to linking the analyzed sites here to the wider outcrop belt. For example, a previously described "mass-flow" facies (Gehling and Droser 2013) was not recognized in this study, but matches the ball-and-pillow structures described in our Facies 4 (Fig. 12A, B, G) (Gehling and Droser 2013). This mass-flow facies reportedly includes *out of situ Nasepia*, *Pteridinium*, and *Rangea* (Gehling and Droser 2013; Laflamme et al. 2018), in addition to detached, folded and stretched *Dickinsonia*, deformation of which is suggested to have occurred during

transportation (Evans et al. 2019). The apparent correlation of deformed horizons between the studied sites here suggests that deformation occurred shortly after deposition, and might have had a seismic trigger (Fig. 23) (e.g., Davies et al. 2005; Owen et al. 2011). However, we are not presently able to determine if this correlation can be extrapolated to the Nilpena site from which the mass-flow facies is most commonly described (Gehling and Droser 2013; Tarhan et al. 2017; Evans et al. 2019). Whilst some fossils at that location have evidently undergone transportation from their life position (Gehling and Droser 2013; Laflamme et al. 2018; Evans et al. 2019), the proposed sub-storm-wave base canyon model for the mass flow events (Gehling and Droser 2013; Tarhan et al. 2017; Droser et al. 2019) is difficult to reconcile with the sequence-stratigraphic framework suggested here. As the sudden liquefaction of large masses of sand is a common phenomenon in a number of paralic environments (e.g., Lowe and Guy 2000; Van den Berg et al. 2002), it is possible that any mass-flow events preserved across the outcrop belt also occurred at more reduced water depths, a speculation that requires future testing.

Other revisions to particular sedimentary facies in this study also provide a more parsimonious regional sequence stratigraphic model for Rawnsley Quartzite deposition (Fig. 23). For example, Reid et al. (2020, p. 333) highlighted that the deposition of their "CLS" facies (formerly sheet flow; Gehling and Droser 2013) in settings beneath maximum wave base did "not account for the rapid base level fluctuations required to increase water depth sufficiently" to enable deposition of their intercalated shallow marine facies (their CS, ORS, and CFRS). Our revised interpretation of CLS as a lower-shoreface deposit (Facies 5) readily accounts for its centimeter-scale intercalation with other shallow-marine deposits.

PALEOBIOLOGICAL IMPLICATIONS

Interpretations of the phylogenic affinities and modes of life of the Ediacaran macrobiota are partially informed by the environments they inhabited, evidence for which is archived as sedimentary facies. In addition to paleobiological reconstructions, correct inferences of paleoenvironmental settings and water depth are essential for assessments of global trends in taxonomic diversity, evolution, and paleoecology (Waggoner 2003; Boag et al. 2016; Muscente et al. 2019). Considering Ediacara Member fossiliferous facies as having been deposited entirely above fair-weather wave base has a number of wider paleobiological implications. On a broad scale, the three biotic "assemblages" of the Ediacaran macrobiota, the Avalon (~ 579–559 Ma), White Sea (558–550 Ma), and Nama (549–541 Ma), have been discussed as having been influenced to greater or lesser degrees by temporal, environmental, and potentially paleogeographic controls (e.g., Waggoner 2003; Boag et al. 2016; Muscente et al. 2019). The Ediacara Member, which is a component of the White Sea assemblage, is widely regarded as recording habitats that represent shallower water depths than the older Avalon assemblage but deeper environments than are typical of the younger Nama assemblage. Our revised shoreface and coastal environmental framework for the Ediacara Member creates significant environmental overlap with some fossil-bearing sections of the Nama assemblages in Namibia (e.g., tidal-flat and shoreface environments interpreted in the fossiliferous Kuibis and Schwarzrand subgroups; Germs 1995; Darroch et al. 2016). This raises the possibility that the biotic turnover apparent in the relatively depauperate Nama assemblage might be more accurately considered as a distinct evolutionary signal, rather than environmental exclusion of particular genera. However, it would be premature to conclude that the Nama assemblage represents a unique faunal stage of Ediacaran evolution until detailed sedimentological studies of Nama-assemblage localities, or more refined global paleogeographic constraints, are obtained.

Fossiliferous White Sea assemblages elsewhere have been interpreted as shoreface settings, including the correlative Vendian Group on the White Sea coast of Russia (Grazdhankin 2004). Significantly, as well as containing biotic assemblages highly comparable to those of the Ediacara Member, these Russian sections are interpreted as lower- and middle-shoreface environments, and contain volumetrically significant quantities of mudrock (Grazdhankin 2004, their Fig. 1). Such fine-grained material is only rarely present in the Ediacara Member (e.g., Liu et al. 2019), representing a negligible component of the shoreface lithologies interpreted for the Ediacara Member (Tarhan et al. 2016). The most parsimonious explanation for the absence of finer-grained material is that Ediacara Member deposition occurred landward of Russian counterpart sections, with mud, presumably present in the active system, bypassing to more distal settings not archived in the studied stratigraphy. If the previously suggested "storm-wave" base depositional environments for Ediacara Member facies (e.g., Gehling 2000; Gehling and Droser 2013; Tarhan et al. 2017; Reid et al. 2020), are to be retained by future researchers, the absence of mudrock in these sections, compared to their supposedly landward Russian counterparts (Grazdhankin 2004), must be accounted for. Future studies should also aim to use consistent nomenclature. In this study (following the widely used scheme of Reading and Collinson (1996)), shoreface environments are considered to extend from the low-tide mark to the fair-weather wave base, offshore environments from the fair-weather wave base to storm-wave base, and shelf environments to water depths below the storm-wave base (Fig. 2). Conversely (as an example), in the global compilation of Ediacaran macrobiota in space and time presented by Boag et al. (2016), the White Sea assemblage is stated to reach "offshore middle shelf" settings (Page 587), despite such settings being considered to occupy bathymetries "well below fair-weather wave base and near storm-wave base" (p. 587). By contrast, previous studies of White Sea assemblages in the Ediacara Member consider three of the five fossiliferous facies as being deposited beneath storm-wave base (e.g., Gehling and Droser 2013, their Fig. 1).

Ediacara Member fossils, which ubiquitously comprise sandstone impressions (e.g., Narbonne 2005), are in effect a distinct subset of the sedimentary surface texture classification defined by Davies et al. (2016). Such sedimentary surface textures develop when a sedimentation system is in stasis, with the insignificant removal or addition of sediment (Tipper 2015; Davies et al. 2017). When undergoing stasis, substrates may be imprinted by a multitude of abiotic and biotic sedimentary surface textures, including those formed by Ediacaran macrobiota. Once preserved in the rock record, these can be defined as "true substrates": "sedimentary bedding planes that demonstrably existed at the sediment–water or sediment air interface at the time of deposition" (Davies and Shillito 2018, p. 679). Ongoing paleoecological research based on bedding-plane analyses must recognize that no two substrates likely preserve the same quantity of stasis. From the moment of exposure, substrates are essentially a blank canvas onto which ecological signals are cumulatively imprinted until the moment of burial: the longer a system is in stasis, the more opportunity for ecological impression. In a recent study, Mitchell et al. (2020) compared community ecology between Avalon and White Sea assemblage Ediacaran bedding planes, the former largely buried by volcaniclastic deposits and the latter by storm events. Distinct processes of burial would have likely resulted in differing amounts of preserved stasis in Avalon and White Sea bedding planes, an additional caveat which should be incorporated into paleoecological work comparing the two assemblages. Similarly, the various Rawnsley Quartzite facies described in this study do not have an equal likelihood of preserving true substrates (and therefore evidence of Ediacaran macrobiota) (Fig. 24). As an example, estuarine channel deposits (Facies 1) only very scarcely contain true substrates (Fig. 6), with the vast majority of beds top-truncated by succeeding strata (Fig. 5A–F). Any net intervals of stasis are consequently lost to erosion, such that it cannot be known with absolute certainty whether the absence of fossils is a genuine environmental signal, or a result of the taphonomic conditions in estuarine facies. Conversely, the vast majority of middle-shoreface (Facies 6) bedding planes are true substrates (Fig. 15),

Facies	Interpretation	True substrates	Macrobiota	Microbial mats
1 & 3	Estuarine/tidally-influenced river	R	A	A
2	Mixed-flat	C	R	R
4	Lagoon?	C	R	R
5	Lower shoreface	C	C	R
6	Middle shoreface	C	C	C
7	Upper shoreface	R	R	A
8	Foreshore	C	A	R
9	Backshore	C	A	A
10	Distributary channels	R	A	A

C Common   R Rare   A Absent

FIG. 24.—Summary of the occurrence of true substrates, macrobiota fossils, and evidence of microbial mats in each described facies of the Ediacara Member and Upper Rawnsley Quartzite.

emphasized by the widespread evidence of former microbial mats which colonized during intervals of little sedimentation (Fig. 15G, H). True substrates are also abundant in foreshore facies (Facies 9) (Figs. 19–21), yet this facies contains very little evidence for Ediacaran macrobiota (the possible exceptions being rare concentric circles tentatively interpreted as holdfasts (Fig. 21B, C)). In this case the absence of Ediacaran macrobiota despite the prevalence of true substrates can be more confidently considered a genuine absence from these intermittently emergent foreshore settings. Furthermore, true substrates may preserve microbially induced sedimentary surface textures (or textured organic surfaces; Gehling and Droser 2009). Such surface textures are often cited as evidence for the ubiquity of organic mats on the Ediacaran seafloor (e.g., Gehling and Droser 2009, 2018; Droser et al. 2017; Tarhan et al. 2017) and are considered to be fundamentally important to Ediacara Member fossil preservation (e.g., Gehling 1999; Narbonne 2005; Liu et al. 2019; though see Tarhan et al. 2016; Bobrovskiy et al. 2019; MacGabhann et al. 2019). However, appreciating that apparently delicate sedimentary surface textures are often an inevitable product of the ordinary interplay of sedimentary stasis and deposition (Davies and Shillito 2018) and require no special preservational circumstances (e.g., protection by microbial mats (e.g., Gehling 2000; Sappenfield et al. 2017; Tarhan et al. 2017)), models of mat-dependent preservation for the Ediacara macrobiota may need reconsideration. This is emphasized by the occurrence of macrobiota fossils on true substrates in Facies 2, 4, and 5, substrates which only very rarely preserve evidence of former microbial mats (Figs. 9H, 12F, 24).

Our findings emphasize that there remains much information to glean from studying the physical environments occupied by the Ediacaran macrobiota. Differences between our interpretations and existing depositional models (e.g., Gehling 2000; Gehling and Droser 2013; Reid et al. 2020) also highlight difficulties in interpreting Precambrian sedimentary strata often missing "smoking-gun" paleontological and ichnological information. Recent studies have recognized the prominent role played by environmental controls on both local (Mitchell et al. 2019) and global (Grazhdankin 2004, 2014; Gehling and Droser 2013; Zakrevskaya 2014; Boag et al. 2016) composition of Ediacaran macrofossil assemblages. Our reinterpretation of the Ediacara Member facies in the central outcrop belt of the Flinders Ranges aligns them far more closely with shoreface facies and similar fossil assemblages of the White Sea region of Russia (e.g., Grazhdankin 2004, their Fig. 5). This revised facies interpretation may also explain the scarcity of certain White Sea taxa in Australia. Our revised paleoenvironmental setting has implications for studies considering the

community dynamics (e.g., Evans et al. 2018) and responses of Ediacaran taxa to environmental disturbance (e.g., Paterson et al. 2017; Reid et al. 2018), which have utilized paleonvironmental interpretations to assist in interpreting paleoecological data.

CONCLUSIONS

The Rawnsley Quartzite in the Central Flinders Ranges is interpreted as an estuarine, shoreface, and coastal succession deposited exclusively above effective (fair-weather) wave base. A complete (idealized) succession consists of amalgamated channelized and cross-bedded sandstones (Facies 1) deposited disconformably above the underlying Chace Quartzite, which pass upwards into ripple-cross-laminated heterolithic sandstones (Facies 2). At certain localities, these facies are overlain either by a thin succession of cross-bedded sandstones (Facies 3) or red silty sandstones (Facies 4). This complex (Facies 1 to 4) is interpreted to record a number of distinct estuarine, intertidal mixed-flat and lagoonal environments containing rare macrofossils. Overlying these coastal deposits are intercalated successions of planar stratified (Facies 5), oscillation-rippled (Facies 6), and multi-directed trough- and planar-cross stratified sandstones (Facies 7). These deposits are considered lower-, middle-, and upper-shoreface deposits respectively, with the former two being highly fossiliferous. Shoreface deposits are vertically succeeded by a thick succession of rippled (Facies 8) and adhered sandstones (Facies 9), interpreted as foreshore and backshore settings respectively. Planar-stratified and cross-stratified sandstones with prevalent ripple cross-lamination (Facies 10) occur towards the top of the Rawnsley Quartzite and are interpreted as the product of distributary channels, occasionally interspersed with lagoon deposits (Facies 4). These refined facies interpretations suggest that previously proposed panoptic facies models for the fossiliferous Ediacara Member overestimate water depth in at least some locations. Although we find no evidence to suggest that the Ediacara Member macroscopic organisms were inhabiting terrestrial environments, they do appear to have been living remarkably close to the shoreline. Furthermore, surface trace fossils in foreshore facies represent the earliest evidence for mobile organisms in intermittently emergent environments. Revised estimates of water depth permit re-evaluation of the paleoecology of the Ediacara Member macrobiota, in addition to detailed comparison with other important global sites. It is vital that future paleoecological research considers the important role of sedimentary stasis in determining which environments are suited to fossil

preservation, since not all Ediacara Member facies appear to have possessed conditions favorable for such preservation.

REFERENCES

ALLEN, G.P., AND POSAMENTIER, H.W., 1994, Transgressive facies and sequence architecture in mixed tide- and wave-dominated incised valleys: example from the Gironde Estuary, France, in Dalrymple, R.W., Boyd, R., and Zaitlin, B.A., eds., Incised-Valley Systems: Origin and Sedimentary Sequences: SEPM, Special Publication 51, p. 225–240.

AMOS, C.L., 1995, Siliciclastic tidal flats, in Perillo, G.M.E., ed., Geomorphology and Sedimentology of Estuaries: Amsterdam, Elsevier, Developments in Sedimentology 53, p. 273–301.

ARNOTT, R.W.C., 1993, Quasi-planar-laminated sandstone beds of the Lower Cretaceous Bootlegger Member, north-central Montana; evidence of combined-flow sedimentation: Journal of Sedimentary Petrology, v. 63, p. 488–494.

BANIAK, G.M., GINGRAS, M.K., BURNS, B.A., AND PEMBERTON, G.S., 2014, An example of a highly bioturbated, storm-influenced shoreface deposit: Upper Jurassic Ula Formation, Norwegian North Sea: Sedimentology, v. 61, p. 1261–1285.

BOAG, T.H., DARROCH, S.A., AND LAFLAMME, M., 2016, Ediacaran distributions in space and time: testing assemblage concepts of earliest macroscopic body fossils: Paleobiology, v. 42, p. 574–594.

BOBKOV, N.I., KOLESNIKOV, A.V., MASLOV, A.V., AND GRAZHDANKIN, D.V., 2019, The occurrence of Dickinsonia in non-marine facies: Estudios Geológicos, v. 75, p. 96.

BOBROVSKIY, I., KRASNOVA, A., IVANTSOV, A., LUZHNAYA, E., AND BROCKS, J.J., 2019, Simple sediment rheology explains the Ediacara biota preservation: Nature Ecology & Evolution, v. 3, p. 582–589.

BOYD, R., FORBES, D.L., AND HEFFLER, D.E., 1988, Time-sequence observations of wave-formed sand ripples on an ocean shoreface: Sedimentology, v. 35, p. 449–464.

BRAAT, L., KESSEL, T.V., LEUVEN, J.R., AND KLEINHANS, M.G., 2017, Effects of mud supply on large-scale estuary morphology and development over centuries to millennia: Earth Surface Dynamics, v. 5, p. 617–652.

BRADLEY, G.M., REDFERN, J., HODGETTS, D., GEORGE, A.D., AND WACH, G.D., 2018, The applicability of modern tidal analogues to pre-vegetation paralic depositional models: Sedimentology, v. 65, p. 2171–2201.

BRADLEY, R.W., AND VENDITTI, J.G., 2017, Reevaluating dune scaling relations: Earth-Science Reviews, v. 165, p. 356–376.

BRÜCKNER, M.Z., BRAAT, L., SCHWARZ, C., AND KLEINHANS, M.G., 2020, What came first, mud or biostabilizers? elucidating interacting effects in a coupled model of mud, saltmarsh, microphytobenthos, and estuarine morphology: Water Resources Research, v. 56, 24 p.

BUATOIS, L.A., SACCAVINO, L.L., AND ZAVALA, C., 2011, Ichnologic signatures of hyperpycnal flow deposits in Cretaceous river-dominated deltas, Austral Basin, southern Argentina, in Slaat, R.M., and Zavala, C., eds., Sediment Transfer from Shelf to Deep Water: Revisiting the Delivery System: American Association of Petroleum Geologists, Studies in Geology 61, p. 153–170.

CALLOW, R.H., AND BRASIER, M.D., 2009, Remarkable preservation of microbial mats in Neoproterozoic siliciclastic settings: implications for Ediacaran taphonomic models: Earth-Science Reviews, v. 96, p. 207–219.

CARROLL, A.R., AND WARTES, M.A., 2003, Organic carbon burial by large Permian lakes, north-west China, in Chan, M.A., and Archer, A.W., eds., Extreme Depositional Environments: Mega End Members in Geologic Time: Geological Society of America, Special Paper 370, p. 91–104.

CARTIGNY, M.J., VENTRA, D., POSTMA, G., AND VAN DEN BERG, J.H., 2014, Morphodynamics and sedimentary structures of bedforms under supercritical-flow conditions: new insights from flume experiments: Sedimentology, v. 61, p. 712–748.

CATUNEANU, O., 2006, Principles of Sequence Stratigraphy: Amsterdam, Elsevier, 375 p.

CHAKRABARTI, A., 2005, Sedimentary structures of tidal flats: a journey from coast to inner estuarine region of eastern India: Journal of Earth System Science, v. 114, p. 353–368.

CLIFTON, H.E., 2003, Supply, segregation, successions, and significance of shallow marine conglomeratic deposits: Bulletin of Canadian Petroleum Geology, v. 51, p. 370–388.

COLLETTE, J.H., HAGADORN, J.W., AND LACELLE, M.A., 2010, Dead in their tracks: Cambrian arthropods and their traces from intertidal sandstones of Quebec and Wisconsin: Palaios, v. 25, p. 475–486.

COUNTS, J.W., RARITY, F., AINSWORTH, R.B., AMOS, K.J., LANE, T., MORON, S., TRAINOR, J., VALENTI, C., AND NANSON, R., 2016, Sedimentological interpretation of an Ediacaran delta: Bonney Sandstone, South Australia: Australian Journal of Earth Sciences, v. 63, p. 257–273.

DALRYMPLE, R.W., ZAITLIN, B.A. AND BOYD, R., 1992, Estuarine facies models; conceptual basis and stratigraphic implications: Journal of Sedimentary Petrology, v. 62, p. 1130–1146.

DARROCH, S.A., BOAG, T.H., RACICOT, R.A., TWEEDT, S., MASON, S.J., ERWIN, D.H., AND LAFLAMME, M., 2016, A mixed Ediacaran–metazoan assemblage from the Zaris Sub-basin, Namibia: Palaeogeography, Palaeoclimatology, Palaeoecology, v. 459, p. 198–208.

DASHTGARD, S.E., MACEACHERN, J.A., FREY, S.E., AND GINGRAS, M.K., 2012, Tidal effects on the shoreface: towards a conceptual framework: Sedimentary Geology, v. 279, p. 42–61.

DAVIES, N.S., AND SHILLITO, A.P., 2018, Incomplete but intricately detailed: the inevitable preservation of true substrates in a time-deficient stratigraphic record: Geology, v. 46, p. 679–682.

DAVIES, N.S., TURNER, P., AND SANSOM, I.J., 2005, Soft-sediment deformation structures in the Late Silurian Stubdal Formation: the result of seismic triggering: Norwegian Journal of Geology/Norsk Geologisk Forening, v. 85, p. 233–243.

DAVIES, N.S., LIU, A.G., GIBLING, M.R., AND MILLER, R.F., 2016, Resolving MISS conceptions and misconceptions: a geological approach to sedimentary surface textures generated by microbial and abiotic processes: Earth-Science Reviews, v. 154, p. 210–246.

DAVIES, N.S., SHILLITO, A.P., AND MCMAHON, W.J., 2017, Short-term evolution of primary sedimentary surface textures (microbial, abiotic, ichnological) on a dry stream bed: modern observations and ancient implications: Palaios, v. 32, p. 125–134.

DAVIES, N.S., SHILLITO, A.P., AND MCMAHON, W.J., 2019, Where does the time go? Assessing the chronostratigraphic fidelity of sedimentary geological outcrops in the Pliocene–Pleistocene Red Crag Formation, eastern England: Geological Society of London, Journal, v. 176, p. 1154–1168.

DAVIES, N.S., SHILLITO, A.P., SLATER, B.J., LIU, A.G., AND MCMAHON, W.J., 2020, Evolutionary synchrony of Earth's biosphere and sedimentary-stratigraphic record: Earth-Science Reviews, v. 201, no. 102979.

DAVIS, R.A., 1978, Beach and nearshore zone, in Davis, R.A., ed., Coastal Sedimentary Environments: Berlin, Springer-Verlag, p. 237–285.

DE RAAF, J.F.M., AND BOERSMA, J.R., 1971, Tidal deposits and their sedimentary structures: Geologie en Mijnbouw, v. 50, p. 479–504.

DOUCETTE, J.S., AND O'DONOGHUE, T., 2006, Response of sand ripples to change in oscillatory flow: Sedimentology, v. 53, p. 581–596.

DROSER, M.L., AND GEHLING, J.G., 2008, Synchronous aggregate growth in an abundant new Ediacaran tubular organism: Science, v. 319, p. 1660–1662.

DROSER, M.L., AND GEHLING, J.G., 2015, The advent of animals: the view from the Ediacaran: National Academy of Sciences (USA), Proceedings, v. 112, p. 4865–4870.

DROSER, M.L., GEHLING, J.G., AND JENSEN, S.R., 2006, Assemblage palaeoecology of the Ediacara biota: the unabridged edition?: Palaeogeography, Palaeoclimatology, Palaeoecology, v. 232, p. 131–147.

DROSER, M.L., TARHAN, L.G., AND GEHLING, J.G., 2017, The rise of animals in a changing environment: global ecological innovation in the late Ediacaran: Annual Review of Earth and Planetary Sciences, v. 45, p. 593–617.

DROSER, M.L., GEHLING, J.G., TARHAN, L.G., EVANS, S.D., HALL, C.M., HUGHES, I.V., HUGHES, E.B., DZAUGIS, M.E., DZAUGIS, M.P., DZAUGIS, P.W., AND RICE, D., 2019, Piecing together the puzzle of the Ediacara Biota: excavation and reconstruction at the Ediacara National Heritage site Nilpena (South Australia): Palaeogeography, Palaeoclimatology, Palaeoecology, v. 513, p. 132–145.

EVANS, S.D., DZAUGIS, P.W., DROSER, M.L., AND GEHLING, J.G., 2018, You can get anything you want from Alice's Restaurant Bed: exceptional preservation and an unusual fossil assemblage from a newly excavated bed (Ediacara Member, Nilpena, South Australia): Australian Journal of Earth Sciences, v. 67, p. 1–11.

EVANS, S.D., HUANG, W., GEHLING, J.G., KISAILUS, D., AND DROSER, M.L., 2019, Stretched, mangled, and torn: responses of the Ediacaran fossil Dickinsonia to variable forces: Geology, v. 47, p. 1049–1053.

FAIRCHILD, I.J., AND HERRINGTON, P.M., 1989, A tempestite–stromatolite–evaporite association (late Vendian, East Greenland): a shoreface–lagoon model: Precambrian Research, v. 43, p. 101–127.

FIELDING, C.R., 2006, Upper flow regime sheets, lenses and scour fills: extending the range of architectural elements for fluvial sediment bodies: Sedimentary Geology, v. 190, p. 227–240.

FRINGS, R.M., 2008, Downstream fining in large sand-bed rivers: Earth-Science Reviews, v. 87, p. 39–60.

GEHLING, J.G., 1982, The sedimentology and stratigraphy of the late Precambrian Pound Subgroup, central Flinders Ranges, South Australia [MS Thesis]: University of Adelaide, South Australia, 112 p.

GEHLING, J.G., 1999, Microbial mats in terminal Proterozoic siliciclastics: Ediacaran death masks: Palaios, v. 14, p. 40–57.

GEHLING, J.G., 2000, Environmental interpretation and a sequence stratigraphic framework for the terminal Proterozoic Ediacara Member within the Rawnsley Quartzite, South Australia: Precambrian Research, v. 100, p. 65–95.

GEHLING, J.G., AND DROSER, M.L., 2009, Textured organic surfaces associated with the Ediacara biota in South Australia: Earth-Science Reviews, v. 96, p. 196–206.

GEHLING, J.G., AND DROSER, M.L., 2013, How well do fossil assemblages of the Ediacara Biota tell time? Geology, v. 41, p. 447–450.

GEHLING, J.G., AND DROSER, M.L., 2018, Ediacaran scavenging as a prelude to predation: Emerging Topics in Life Sciences, v. 2, p. 213–222.

GERMS, G.J., 1995, The Neoproterozoic of southwestern Africa, with emphasis on platform stratigraphy and paleontology: Precambrian Research, v. 73, p. 137–151.

GLAESSNER, M.F., AND DAILY, B., 1959, The geology and Late Precambrian fauna of the Ediacara fossil reserve: Records of the South Australian Museum, v. 13, p. 369–401.

GRAZHDANKIN, D., 2004, Patterns of distribution in the Ediacaran biotas: facies versus biogeography and evolution: Paleobiology, v. 30, p. 203–221.

GRAZHDANKIN, D., 2014, Patterns of evolution of the Ediacaran soft-bodied biota: Journal of Paleontology, v. 88, p. 269–283.

GREY, K., AND CALVER, C.R., 2007, Correlating the Ediacaran of Australia, *in* Vickers-Rich, and Komarower, O., eds., The rise and fall of the Ediacaran Biota: Geological Society of London, Special Publication 286, p. 115–135.

HAGADORN, J.W., COLLETTE, J.H., AND BELT, E.S., 2011, Eolian–aquatic deposits and faunas of the middle Cambrian Potsdam Group: Palaios, v. 26, p. 314–334.

HARAZIM, D., CALLOW, R.H., AND MCILROY, D., 2013, Microbial mats implicated in the generation of intrastratal shrinkage ("synaeresis") cracks: Sedimentology, v. 60, p. 1621–1638.

HILL, P.R., MEULÉ, S., AND LONGUÉPÉE, H., 2003, Combined-flow processes and sedimentary structures on the shoreface of the wave-dominated Grande-Riviere-de-la-Baleine delta: Journal of Sedimentary Research, v. 73, p. 217–226.

JENKINS, R.J.F., 1975, An environmental study of the rocks containing the Ediacara assemblage in the Flinders Ranges [Abstract]: 1st Australian Geological Convention, Adelaide, Geological Society of Australia, Abstracts, p. 21–22.

JENKINS, R.J.F., FORD, C.H., AND GEHLING, J.G., 1983, The Ediacara member of the Rawnsley quartzite: the context of the Ediacara assemblage (late Precambrian, Flinders Ranges): Geological Society of Australia, Journal, v. 30, p. 101–119.

JULIEN, P.Y., KLAASSEN, G.J., TEN BRINKE, W.B.M., AND WILBERS, A.W.E., 2002, Case study: bed resistance of Rhine River during 1998 flood: Journal of Hydraulic Engineering, v. 128, p. 1042–1050.

KLEINHANS, M.G., 2010, Sorting out river channel patterns: Progress in Physical Geography, v. 34, p. 287–326.

KLEINHANS, M.G., VAN DER VEGT, M., VAN SCHELTINGA, R.T., BAAR, A.W., AND MARKIES, H., 2012, Turning the tide: experimental creation of tidal channel networks and ebb deltas: Netherlands Journal of Geosciences, v. 91, p. 311–323.

KLEINHANS, M.G., VAN SCHELTINGA, R.T., VAN DER VEGT, M., AND MARKIES, H., 2015, Turning the tide: growth and dynamics of a tidal basin and inlet in experiments: Journal of Geophysical Research, Earth Surface, v. 120, p. 95–119.

KNOLL, A.H., WALTER, M.R., NARBONNE, G.M., AND CHRISTIE-BLICK, N., 2004, A new period for the geologic time scale: Science, v. 305, p. 621.

KNOLL, A.H., WALTER, M.R., NARBONNE, G.M., AND CHRISTIE-BLICK, N., 2006, The Ediacaran Period: a new addition to the geologic time scale: Lethaia v. 39, p. 13–30.

KOEHN, D., BONS, P., MONTANARI, M., AND SEILACHER, A., 2014, The elastic age: rise and fall of Precambrian biomat communities [Abstract]: European Geosciences Union, General Assembly Conference, Abstract 16, Vienna.

LAFLAMME, M., GEHLING, J.G., AND DROSER, M.L., 2018, Deconstructing an Ediacaran frond: three-dimensional preservation of Arborea from Ediacara, South Australia, Journal of Paleontology, v. 92, p. 323–335.

LECLAIR, S.F., AND BRIDGE, J.S., 2001, Quantitative interpretation of sedimentary structures formed by river dunes: Journal of Sedimentary Research, v. 71, p. 713–716.

LEUVEN, J.R.F.W., KLEINHANS, M.G., WEISSCHER, S.A.H., AND VAN DER VEGT, M., 2016, Tidal sand bar dimensions and shapes in estuaries: Earth-Science Reviews, v. 161, p. 204–223.

LINNEMANN, U., OVTCHAROVA, M., SCHALTEGGER, U., GÄRTNER, A., HAUTMANN, M., GEYER, G., VICKERS-RICH, P., RICH, T., PLESSEN, B., HOFMANN, M., AND ZIEGER, J., 2019, New high-resolution age data from the Ediacaran–Cambrian boundary indicate rapid, ecologically driven onset of the Cambrian explosion: Terra Nova, v. 31, p. 49–58.

LIU, A.G., AND DUNN, F.S., 2020, Filamentous connections between Ediacaran fronds: Current Biology, v. 30, p. 1322–1328.

LIU, A.G., MCILROY, D., MATTHEWS, J.J., AND BRASIER, M.D., 2012, A new assemblage of juvenile Ediacaran fronds from the Drook Formation, Newfoundland: Geological Society of London, Journal, v. 169, p. 395–403.

LIU, A.G., KENCHINGTON, C.G., AND MITCHELL, E.G., 2015, Remarkable insights into the paleoecology of the Avalonian Ediacaran macrobiota: Gondwana Research, v. 27, p. 1355–1380.

LIU, A.G., MCMAHON, S., MATTHEWS, J.J., STILL, J.W., AND BRASIER, A.T., 2019, Petrological evidence supports the death mask model for the preservation of Ediacaran soft-bodied organisms in South Australia: Geology, v. 47, p. 215–218.

LONG, D.G.F., 2011, Architecture and depositional style of fluvial systems before land plants: a comparison of Precambrian, early Paleozoic and modern river deposits, *in* Davidson, S., Leleu, S., and North, C.P., eds., From River to Rock Record: The Preservation of Fluvial Sediments and Their Subsequent Interpretation: SEPM, Special Publication 97, p. 37–61.

LOWE, D.R., AND GUY, M., 2000, Slurry-flow deposits in the Britannia Formation (Lower Cretaceous), North Sea: a new perspective on the turbidity current and debris flow problem: Sedimentology, v. 47, p. 31–70.

MACEACHERN, J.A., BANN, K.L., 2008, The role of ichnology in refining shallow marine facies models, *in* Hampson, G.J., Steel, R.J., Burgess, P.M., and Dalrymple, R.W., eds., Recent Advances in Models of Siliciclastic Shallow-Marine Stratigraphy: SEPM, Special Publication 90, p. 73–116.

MACGABHANN, B.A., SCHIFFBAUER, J.D., HAGADORN, J.W., VAN ROY, P., LYNCH, E.P., MORRISON, L., AND MURRAY, J., 2019, Resolution of the earliest metazoan record: differential taphonomy of Ediacaran and Paleozoic fossil molds and casts: Palaeogeography, Palaeoclimatology, Palaeoecology, v. 513, p. 146–165.

MACNAUGHTON, R.B., COLE, J.M., DALRYMPLE, R.W., BRADDY, S.J., BRIGGS, D.E., AND LUKIE, T.D., 2002, First steps on land: arthropod trackways in Cambrian–Ordovician eolian sandstone, southeastern Ontario, Canada: Geology, v. 30, p. 391–394.

MACNAUGHTON, R.B., HAGADORN, J.W., AND DOTT, R.H., 2019, Cambrian wave-dominated tidal-flat deposits, central Wisconsin, USA: Sedimentology, v. 66, p. 1643–1672.

MARTENS, J.H., 1931, Persistence of feldspar in beach sand: American Mineralogist, Journal of Earth and Planetary Materials, v. 16, p. 526–531.

MARTIN, M.W., GRAZHDANKIN, D.V., BOWRING, S.A., EVANS, D.A.D., FEDONKIN, M.A., AND KIRSCHVINK, J.L., 2000, Age of Neoproterozoic bilatarian body and trace fossils, White Sea, Russia: implications for metazoan evolution: Science, v. 288, p. 841–845.

MARTINIUS, A.W., AND VAN DEN BERG, J.H., 2011, Atlas of Sedimentary Structures in Estuarine and Tidally-Influenced River Deposits of the Rhine–Meuse–Scheldt System: Their Application to the Interpretation of Analogous Outcrop and Subsurface Depositional Systems: Houten, European Association of Geoscientists and Engineers, Pblications, 298 p.

MATTHEWS, J.J., LIU, A.G., YANG, C., MCILROY, D., LEVELL, B., AND CONDON, D.J., 2020, A chronostratigraphic framework for the rise of the Ediacaran Macrobiota: new constraints from Mistaken Point Ecological Reserve, Newfoundland: Geological Society of America, Bulletin, doi:10.1130/B35646.1.

MCMAHON, W.J., AND DAVIES, N.S., 2018a, Evolution of alluvial mudrock forced by early land plants: Science, v. 359, p. 1022–1024.

MCMAHON, W.J., AND DAVIES, N.S., 2018b, High-energy flood events recorded in the Mesoproterozoic Meall Dearg Formation, NW Scotland: their recognition and implications for the study of pre-vegetation alluvium: Geological Society of London, Journal, v. 175, p. 13–32.

MCMAHON, S., VAN SMEERDIJK HOOD, A., AND MCILROY, D., 2017a, The origin and occurrence of subaqueous sedimentary cracks: Geological Society of London, Special Publication 448, p. 285–309.

MCMAHON, W.J., DAVIES, N.S., AND WENT, D.J., 2017b, Negligible microbial matground influence on pre-vegetation river functioning: evidence from the Ediacaran–Lower Cambrian Series Rouge, France: Precambrian Research, v. 292, p. 13–34.

MENZIES, J., 1990, Sand intraclasts within a diamicton mélange, southern Niagara Peninsula, Ontario, Canada: Journal of Quaternary Science, v. 5, p. 189–206.

MIALL, A.D., 1996, The Geology of Fluvial Deposits: New York, Springer-Verlag, 582 p.

MIALL, A.D., 2015, Updating uniformitarianism: stratigraphy as just a set of "frozen accidents," *in* Smith, D.G., Bailey, R.J., Burgess, P., and Fraser, A., eds., Strata and Time: Geological Society of London, Special Publication 404, p. 11–36.

MITCHELL, E.G., AND BUTTERFIELD, N.J., 2018, Spatial analyses of Ediacaran communities at Mistaken Point: Paleobiology, v. 44, p. 40–57.

MITCHELL, E.G., HARRIS, S., KENCHINGTON, C.G., VIXSEBOXSE, P., ROBERTS, L., CLARK, C., DENNIS, A., LIU, A.G., AND WILBY, P.R., 2019, The importance of neutral over niche processes in structuring Ediacaran early animal communities: Ecology Letters, v. 22, p. 2028–2038.

MITCHELL, E.G., BOBKOV, N., BYKOVA, N., DHUNGANA, A., KOLESNIKOV, A.V., HOGARTH, I.R., LIU, A.G., MUSTILL, T.M., SOZONOV, N., ROGOV, V.I., AND XIAO, S., 2020, The influence of environmental setting on the community ecology of Ediacaran organisms: Interface Focus, v. 10, no. 20190109.

MUSCENTE, A.D., BYKOVA, N., BOAG, T.H., BUATOIS, L.A., MÁNGANO, M.G., ELEISH, A., PRABHU, A., PAN, F., MEYER, M.B., SCHIFFBAUER, J.D., FOX, P., HAZEN, R.M., AND KNOLL, A.H., 2019, Ediacaran biozones identified with network analysis provide evidence for pulsed extinctions of early complex life: Nature Communications, v. 10, p. 1–15.

NARBONNE, G.M., 2005, The Ediacara biota: Neoproterozoic origin of animals and their ecosystems: Annual Reviews of Earth and Planet Science, v. 33, p. 421–442.

NORTH, C.P., AND DAVIDSON, S.K., 2012, Unconfined alluvial flow processes: recognition and interpretation of their deposits, and the significance for palaeogeographic reconstruction: Earth-Science Reviews, v. 111, p. 199–223.

OWEN, G., MORETTI, M., AND ALFARO, P., 2011, Recognising triggers for soft-sediment deformation: current understanding and future directions: Sedimentary Geology, v. 235, p. 133–140.

PASSCHIER, S., AND KLEINHANS, M.G., 2005, Observations of sand waves, megaripples, and hummocks in the Dutch coastal area and their relation to currents and combined flow conditions: Journal of Geophysical Research, Earth Surface, v. 110, no. F04S15.

PATERSON, J.R., GEHLING, J.G., DROSER, M.L., AND BICKNELL, R.D., 2017, Rheotaxis in the Ediacaran epibenthic organism Parvancorina from South Australia: Scientific Reports, v. 7, no. 45539.

PEMBERTON, S.G., MACEACHERN, J.A., DASHTGARD, S.E., BANN, K.L., GINGRAS, M.K., AND ZONNEVELD, J.P., 2012, Shorefaces, *in* Knaust, D.K., and Bromley, R.G., Trace Fossils as Indicators of Sedimentary Environments: Amsterdam, Elsevier, Developments in Sedimentology 64, p. 563–603.

PFLÜGER, F., AND GRESSE, P.G., 1996, Microbial sand chips: a non-actualistic sedimentary structure: Sedimentary Geology, v. 102, p. 263–274.

POSTMA, G., ROEP, T.B., AND RUEGG, G.H., 1983, Sandy–gravelly mass-flow deposits in an ice-marginal lake (Saalian, Leuvenumsche Beek Valley, Veluwe, The Netherlands), with emphasis on plug-flow deposits: Sedimentary Geology, v. 34, p. 59–82.

PRAVE, A.R., 2002, Life on land in the Proterozoic: evidence from the Torridonian rocks of northwest Scotland: Geology, v. 30, p. 811–814.

QUINN, J.G., 2011, Is most hummocky cross-stratification formed by large-scale ripples?: Sedimentology, v. 58, p. 1414–1433.

READING, H.G., AND COLLINSON, J.D., 1996, Clastic coasts, *in* Reading, H.G., ed., Sedimentary Environments: Processes, Facies and Stratigraphy, 3rd Edition: Oxford, Blackwell Science, p. 154–231.

REID, L.M., HOLMES, J.D., PAYNE, J.L., GARCÍA-BELLIDO, D.C., AND JAGO, J.B., 2018, Taxa, turnover and taphofacies: a preliminary analysis of facies-assemblage relationships in the Ediacara Member (Flinders Ranges, South Australia): Australian Journal of Earth Sciences, p. 1–10.

REID, L.M., PAYNE, J.L., GARCÍA-BELLIDO, D.C., AND JAGO, J.B., 2020, The Ediacara Member, South Australia: lithofacies and palaeoenvironments of the Ediacara biota: Gondwana Research, v. 80, p. 321–334.

REID, P., AND PREISS, W., 1999, Parachilna map sheet: South Australian Geological Survey, Geological Atlas, v. 1, no. 54e13.

REINECK, H.E., AND SINGH, I.B., 1980, Depositional Sedimentary Environments: Berlin, Springer-Verlag, 551 p.

REINSON, G.E., 1984, Barrier-Island and associated strand-plain systems, *in* Walker, R., ed., Facies Models, 2nd Edition: Kitchener, Ainsworth, p. 117–133.

RETALLACK, G.J., 2012, Were Ediacaran siliciclastics of South Australia coastal or deep marine?: Sedimentology, v. 59, p. 1208–1236.

RETALLACK, G.J., 2013, Ediacaran life on land: Nature, v. 493, p. 89–92.

SAPPENFIELD, A.D., TARHAN, L.G., AND DROSER, M.L., 2017, Earth's oldest jellyfish strandings: a unique taphonomic window or just another day at the beach?: Geological Magazine, v. 154, p. 859–874.

SARKAR, S., AND BANERJEE, S., 2020, Facies, paleogeography and sequence stratigraphy, *in* Sarkar, S., and Banerjee, S., eds., A Synthesis of Depositional Sequence of the Proterozoic Vindhyan Supergroup in Son Valley, Singapore: Springer, p. 31–104.

SARKAR, S., SAMANTA, P., AND ALTERMANN, W., 2011, Setulfs, modern and ancient: formative mechanism, preservation bias and palaeoenvironmental implications: Sedimentary Geology, v. 238, p. 71–78.

SEILACHER, A., 2008, Biomats, biofilms, and bioglue as preservational agents for arthropod trackways: Palaeogeography, Palaeoclimatology, Palaeoecology, v. 270, p. 252–257.

SHILLITO, A.P., AND DAVIES, N.S., 2018, Death near the shoreline, not life on land: Ordovician arthropod trackways in the Borrowdale Volcanic Group, UK: Geology, v. 47, p. 55–58.

SHILLITO, A.P., AND DAVIES, N.S., 2020, The Tumblagooda Sandstone revisited: exceptionally abundant trace fossils and geological outcrop provide a window onto Palaeozoic littoral habitats before invertebrate terrestrialization: Geological Magazine, p. 1–32, doi:10.1017/S0016756820000199.

SOZONOV, N.G., BOBKOV, N.I., MITCHELL, E.G., KOLESNIKOV, A.V., AND GRAZHDANKIN, D.V., 2019, The ecology of *Dickinsonia* on tidal flats: Estudios Geológicos, v. 75, no. e116.

SPRIGG, R.C., 1947, Early Cambrian(?) jellyfishes from the Flinders Ranges, South Australia: Royal Society of South Australia, Transactions, v. 71, p. 212–224.

SUTER, J.R., 2006, Facies models revisited: clastic shelves, *in* Posamentier, H.W., and Walker, R.G., eds., Facies Models Revisited: SEPM, Special Publication 84, p. 339–397.

TANOLI, S.K., AND PICKERILL, R.K., 1990, Lithofacies and basinal development of the type "Etcheminian Series" (Lower Cambrian Ratcliffe Brook Formation), Saint John area, southern New Brunswick: Atlantic Geology, v. 26, p. 57–78.

TARHAN, L.G., DROSER, M.L., AND GEHLING, J.G., 2015, Depositional and preservational environments of the Ediacara Member, Rawnsley Quartzite (South Australia): assessment of paleoenvironmental proxies and the timing of "ferruginization": Palaeogeography, Palaeoclimatology, Palaeoecology, v. 434, p. 4–13.

TARHAN, L.G., HOOD, A.V., DROSER, M.L., GEHLING, J.G., AND BRIGGS, D.E., 2016, Exceptional preservation of soft-bodied Ediacara Biota promoted by silica-rich oceans: Geology, v. 44, p. 951–954.

TARHAN, L.G., DROSER, M.L., GEHLING, J.G., AND DZAUGIS, M.P., 2017, Microbial mat sandwiches and other anactualistic sedimentary features of the Ediacara Member (Rawnsley Quartzite, South Australia): implications for interpretation of the Ediacaran sedimentary record: Palaios, v. 32, p. 181–194.

TIPPER, J.C., 2015, The importance of doing nothing: stasis in sedimentation systems and its stratigraphic effects, *in* Smith, D.G., Bailey, R.J., Burgess, P., and Fraser, A., eds., Strata and Time: Probing the Gaps in our Understanding: Geological Society of London, Special Publication 404, p. 105–122.

TIRSGAARD, H., AND ØXNEVAD, I.E., 1998, Preservation of pre-vegetational mixed fluvio–aeolian deposits in a humid climatic setting: an example from the Middle Proterozoic Eriksfjord Formation, Southwest Greenland: Sedimentary Geology, v. 120, p. 295–317.

VAIL, P.R., HARDENBOL, J., AND TODD, R.G., 1984, Jurassic unconformities, chronostratigraphy, and sea-level changes from seismic stratigraphy and biostratigraphy: American Association of Petroleum Geologists, v. 36, p. 129–144.

VAN DE LAGEWEG, W.I., BRAAT, L., PARSONS, D.R., AND KLEINHANS, M.G., 2018, Controls on mud distribution and architecture along the fluvial-to-marine transition: Geology, v. 46, p. 971–974.

VAN DE LAGEWEG, W.I., VAN DIJK, W.M., BOX, D., AND KLEINHANS, M.G., 2016, Archimetrics: a quantitative tool to predict three-dimensional meander belt sandbody heterogeneity: SEPM, The Depositional Record, v. 2, p. 22–46.

VAN DEN BERG, J.H., VAN GELDER, A., AND MASTBERGEN, D.R., 2002, The importance of breaching as a mechanism of subaqueous slope failure in fine sand: Sedimentology, v. 49, p. 81–95.

WAGGONER, B., 2003, The Ediacaran biotas in space and time: Integrative and Comparative Biology, v. 43, p. 104–113.

WALKER, R.G., AND PLINT, A.G., 1992, Wave-and storm-dominated shallow marine system, *in* Walker, R.G., and James, N.P., eds., Facies Models: Response to Sea Level Change: Geological Association of Canada, p. 219–238.

WALTHER, J., 1894, Einleitung in die Geologie als historische Wissenschaft, *in* Lithogenesis der Gegenwart: Jena, G. Fischer, v. 3, p. 535–1055

WENT, D.J., 2013, Quartzite development in early Palaeozoic nearshore marine environments: Sedimentology, v. 60, p. 1036–1058.

ZAKREVSKAYA, M., 2014, Paleoecological reconstruction of the Ediacaran benthic macroscopic communities of the White Sea (Russia): Palaeogeography, Palaeoclimatology, Palaeoecology, v. 410, p. 27–38.